Olga V. Klyubina

Asymptotic methods in ultrasound tomography

2005

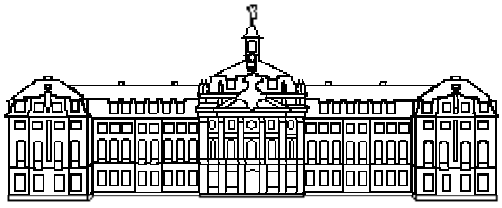

Universität Münster

Angewandte Mathematik

Asymptotic methods in ultrasound tomography

Inaugural-Dissertation
zur Erlangung des Doktorgrades der Naturwissenschaften
im Fachbereich Mathematik und Informatik
der Mathematisch-Naturwissenschaftlichen Fakultät
der Westfälischen Wilhelms-Universität Münster

vorgelegt von

Olga V. Klyubina
aus St.-Petersburg
- 2005 -

Dekan:	Prof. Dr. K. Hinrichs
Erster Gutachter:	Prof. Dr. Dr. h. c. F.Natterer
Zweiter Gutachter:	Prof. Dr. A.Arnold
Tag der mündlichen Prüfung:	14.11.2005
Tag der Promotion:	08.02.2006

To my parents.

Contents

Notations **11**

1 Introduction **13**
1.1 Introduction 13
1.2 Overview 14

2 Helmholtz equation **17**
2.1 Radiation condition 17
2.2 Unique solvability of the direct scattering problem 18
2.2.1 The direct scattering problem 18
2.2.2 Uniqueness 19
2.2.3 Existence of the solution 20
2.3 Examples 22
2.3.1 Scattering on a homogeneous disk 22
2.3.2 Scattering on two concentric disks 28

3 The eikonal approximation **31**
3.1 The asymptotic expansion 31
3.2 The eikonal approximation 32
3.3 The eikonal equation and rays 33
3.4 Ray coordinates and the transport equation 35
3.5 Examples of a ray tracing 38
3.5.1 Scattering on a homogeneous disk 38
3.5.2 Luneberg Lens 40
3.5.3 Simulated data 41
3.5.4 Some remarks 43
3.6 Caustics 44
3.7 An example of a caustic 46

4 Error estimates **49**
4.1 The Burq's 1/k estimate 49

4.2 1/k estimate: initial-value approach 51
4.2.1 Homogeneous medium 51
4.2.2 Nonhomogeneous medium 55
4.3 Error estimate for the eikonal approximation 60

5 Perturbed refractive index **63**
5.1 Hamiltonian treatment 63
5.2 Perturbation of the eikonal function 65

6 Ultrasound tomography **69**
6.1 The inverse scattering problem 69
6.2 Reconstruction methods for a constant background 72
6.3 Reconstruction of the perturbation of refractive index 76
6.4 Numerical examples 78

Bibliography **86**

Notations

$\mathbb{N}$	natural numbers
$\mathbb{N}_0$	$\mathbb{N} \cup \{0\}$
$\mathbb{R}$	real numbers
$\mathbb{R}^+$	real positive numbers
$\mathbb{R}^2$	Euclidean space with points $\mathbf{x} = (x_1, x_2)$, $x_j \in \mathbb{R}$, $\lvert\mathbf{x}\rvert = \sqrt{x_1^2 + x_2^2}$
$\overline{\Omega}$	closure of a set $\Omega \subset \mathbb{R}^2$
$\partial\Omega$	boundary of Ω
$B(R)$	$\{\mathbf{x} \in \mathbb{R}^N : \lvert\mathbf{x}\rvert < R\}$ open ball with radius $R > 0$
$S(R)$	$\{\mathbf{x} \in \mathbb{R}^N : \lvert\mathbf{x}\rvert = R\}$ sphere of a radius $R > 0$
∇u	$(\partial u/\partial x_1, \partial u/\partial x_2)$ gradient of a function $u(\mathbf{x})$
Δu	$(\partial u/\partial x_1)^2 + (\partial u/\partial x_2)^2$ Laplacian of a function $u(\mathbf{x})$
$supp(u)$	support of a function u, the closure of the set $\{\mathbf{x} : u(\mathbf{x}) \neq 0\}$
$\widehat{f}(\xi)$	$(1/\sqrt{2\pi}) \int_{\mathbb{R}} \exp(-ix\xi) f(x) dx$ the Fourier transform of $f(x)$
$\widetilde{f}(x)$	$(1/\sqrt{2\pi}) \int_{\mathbb{R}} \exp(ix\xi) f(\xi) d\xi$ the inverse Fourier transform of $f(\xi)$
$C(\overline{\Omega})$	Banach space of continuous functions on $\overline{\Omega}$ with the norm $\lvert\lvert\varphi\rvert\rvert_{\infty,\Omega} = \sup_{\mathbf{x}\in\Omega} \lvert\varphi(\mathbf{x})\rvert$
$C^{0,\gamma}(\Omega)$	with $0 < \gamma < 1$ Banach space of bounded, uniformly Hölder continuous functions φ on Ω with the norm $\lvert\lvert\varphi\rvert\rvert_{0,\gamma,\Omega} = \sup_{\mathbf{x}\in\Omega} \lvert\varphi(\mathbf{x})\rvert + \sup_{\substack{\mathbf{x},\mathbf{y}\in\Omega \\ \mathbf{x}\neq\mathbf{y}}} \frac{\lvert\varphi(\mathbf{x})-\varphi(\mathbf{y})\rvert}{\lvert\mathbf{x}-\mathbf{y}\rvert^\gamma}$
$C^m(\Omega)$	set of functions on Ω having all derivatives up to order $m \in \mathbb{N}$ continuous in Ω

$C^m(\overline{\Omega})$	set of functions in $C^m(\Omega)$ all of those derivatives up to order $m \in \mathbb{N}$ have continuous extensions to $\overline{\Omega}$, it is a Banach space with the norm $\|\|f\|\|_{C^m(\overline{\Omega})} = \max\limits_{\mathbf{x}\in\overline{\Omega}} \max\limits_{\substack{k\leq m \\ j=1,2}} \frac{\partial^k f}{\partial x_j^k}$
$C_0^m(\Omega)$	set of functions on $C^m(\Omega)$ with compact support in Ω
$C^\infty(\Omega)$	$\bigcap\limits_{m=1}^{\infty} C^m(\Omega)$
$L^p(\Omega)$	set of measurable functions on Ω with $1 \leq p < \infty$ and the norm $\|\|f\|\|_p = \left(\int_\Omega \|f(\mathbf{x})\|^p d\mathbf{x}\right)^{1/p} < \infty$
$L_\rho^p(\Omega)$	the weighted space with the norm $\|\|f\|\|_{L_p^\rho} = \|\|((1 + \|\mathbf{x}\|^2)^{1/2})^\rho f\|\|_{L^p}$
D^α	$(\partial/\partial x_1)^{\alpha_1}(\partial/\partial x_2)^{\alpha_2}$ for $\alpha = (\alpha_1, \alpha_2)$
$\|\alpha\|$	for $\alpha = (\alpha_1, \alpha_2)$ $\|\alpha\| = \alpha_1 + \alpha_2$
$H^2(\Omega)$	Sobolev space of functions from $L_2(\Omega)$ all of whose weak derivatives up to order 2 exist and are in $L_2(\Omega)$ with the norm $\|\|f\|\|_{H^2(\Omega)} = \sum\limits_{\|\alpha\|\leq 2} \|\|D^\alpha f\|\|_{L^2(\Omega)}$

Chapter 1

Introduction

1.1 Introduction

Tomography is a name for a collection of methods used for image reconstructions based on projections of an object. With the increase of the computing power the methods became usable in practice and have been used in medical imaging since the early 70's. The tomographic techniques are based on either penetrating radiation which is sent from a set of active sensors through the object or on passive sensors recording signals emitted from inside of the object. Ultrasound is a type of penetrating radiation which is widely used in medical applications nowadays. Ultrasound is usually defined to be sound with frequencies above the limit of human hearing, i.e., above 20 kHz.

Speaking about the history of the development of ultrasound and its applications we should mention Rayleigh who described sound wave in terms of a mathematical equation in his famous book "The Theory of Sound" [Rayleigh1945] first published in 1877. This was a basis for further theoretical work in acoustics. From the experimental side, sound waves with high frequency were first generated by English scientist Galton in 1876, by means of his invention, the Galton whistle. The real breakthrough in the evolution of high frequency echo-sounding techniques came after the piezoelectric effect in certain crystals was discovered by brothers P. and J.Curie in 1880.

The principle of the ultrasound tomography is that ultrasound pulses are transmitted through the object to be imaged. These pulses received on the opposite side of the object will be changed (attenuated and delayed), corresponding to the properties of the object (specifically speed of sound in the object).

Ultrasound has quite a lot of technological applications. The latter include medical imaging, geophysics [Pintavirooj2004], robotic vision [Bolomey1989] etc.

As we already mentioned in ultrasound tomography one has to do with the propagating of the high-frequent wave field in a nonhomogeneous media. Despite of numerous investigations the image reconstruction (preciesly, the reconstruction of the sound speed in the object or, equivalently the refractive index) for this case is still a challenge. In this thesis we propose a new reconstruction method for the ultrasound tomography. This method is based on approximation of the geometrical optic which is valid in the high-frequent case.

1.2 Overview

We begin in the Chapter 2 with the *Helmholtz equation* (2.1) which describes the propagation of the time-harmonic acoustic waves. Adding the *radiation condition* (2.2) to it we state the *direct scattering problem*. The latter has been already detailed studied (see, e.g. [Colton1992, Hähner1998, Hörmander1994]). By use of *Rellich's lemma* 2.2.2 and the *unique continuation principle* 2.2.3 it is proven that the problem has at most one solution. Such a solution (if any) can be represented with the help of the *Lippmann-Schwinger* equation (2.2.3), which is an Fredholm integral equation of the second kind. It follows that the equation has a unique solution if it has a trivial nullspace. Since the problem has at most one solution it is the case. Thus, the direct scattering problem is uniquely solvable.

Unfortunately the analytical solution of the problem exists only in bare handful of cases. In the Section 2.3 we present three of them: propagation of the plane wave in the free space, scattering on a homogeneous disk and on two concentric disks (see, e.g. [Wübbeling1994]). These examples are basically used to test our reconstruction algorithm thereafter.

The reconstruction algorithm is based on the *eikonal approximation* (3.4), which is presented in the Chapter 3. The eikonal approximation is a well-known approximation of the geometrical optics, which is valid in the case when the wave length is smaller than all characteristic geometrical scales of the problem, i.e, the wave number k is large (see, e.g., [Babich1991, Babich1979, Born1999]). In the Section 3.5 we show some examples of ray propagation, i.e., the *ray tracing*, for different media. These examples illustrate that the ray family may have singularities: rays may intersect, focus or have an envelope. Such singularities of a ray family, the *caustics*, (see, e.g., [Bruns1895, Babich1991, Kravtsov1999]) are considered

in the Section 3.6. In the neighbourhood of a caustic the amplitude formally is infinite hence the eikonal approximation is not valid there. Nevertheless comparing the exact solution computed in the Section 2.3 with the corresponding ray tracing we conclude that the exact ray field becomes strong in the neighbourhood of a caustic. In the region near a caustic one should use other type of asymptotic expansions for the wave field (see, e.g., [Kravtsov1999, Babich1979, Vainberg1989]). To avoid the caustic problem we will suppose in this thesis that in the region of interest the ray family has no singularities.

The first problem to solve is: How good is the eikonal approximation in the region of its validity? Thus, we need an estimate of the difference between the eikonal approximation and the exact solution of the Helmholtz equation, which satisfies radiation condition, in terms of the asymptotic parameter $1/k$. This question leads to the problem of finding an estimate of the solution of the inhomogeneous Helmholtz equation in terms of $1/k$. This problem was studied by Vainberg [Vainberg1975] and Burq [Burq2002], who estimated the resolvent of the Helmholtz operator assuming the *non trapping condition* (see, e.g., [Pauen2000]). We present a new proof naturally connected to the question. If we consider the difference between the eikonal approximation and the exact solution of the Helmholtz equation we see that it satisfies an *initial-value problem* for the Helmholtz equation. Although the initial-value problem is unstable, the stabilized versions of it can be developed and actually used in numerical applications (see, e.g., [Natterer1995, Natterer2004]). Using the initial-value problem approach we get the estimate for the solution of the Helmholtz equation and apply it in the Section 4.3 to get the estimate for the eikonal approximation.

In the Chapter 5 we turn to a different problem connected to the direct scattering problem. Suppose that the refractive index of the medium under consideration is a small perturbation of a known one. If it is the case, one can express the perturbed eikonal function in terms of the non perturbed one and the integral of the perturbation over the non perturbed rays (5.1). The expansion (5.1), heuristic derived in, e.g., [Farra1987], is widely used in seismology [Snieder1992, Cerveny1982], but it never was rigorously proven. In Section 5.2 we give the formal proof of this approximation and give an error estimate of it.

The Chapter 6 is devoted to the ultrasound tomography, where the refractive index is unknown. The task is to reconstruct it from the knowledge of the scattered field measured by detectors. We start with the *inverse scattering problem* 6.1. The uniqueness for the problem was stated by Nachmann [Nachman1988]. Many reconstruction algorithms have been proposed, most of them are based on the *Born* and *Rytov approximations* (see, e.g.,

[Kak1988, Devaney]). The case with large values of the wave number k is still a challenge. Up to now the only class of reconstruction algorithms to handle with this case is based on the *propagation-backpropagation mathod* introduced by Natterer and Wübbelling (see, e.g. [Natterer1995, Caponnetto1998, Natterer2004]). We propose a new reconstruction algorithm after the Palamodov's idea ([Palamodov1996]) for the case of large k, which is based directly on the eikonal approximation (3.4).

Acknowledgements

First of all, I would like to thank my advisor Prof. Dr. Dr. h. c. F. Natterer for all the work he has been doing to help me finish this thesis. I am grateful to Dr. F. Wübbeling and Prof. Dr. A.P. Kiselev for fruitful discussions during my work. Also I want to thank Dr. Sh.Amirashvili and Mrs. S. Gurevich for their reading of the thesis as well as for helpful advises.

At last I want to express the most important acknowledgement. I would like to thank my parents as well as Ingeborg Witz and Thomas Fickenscher for invaluable support and encouragement.

Chapter 2

Helmholtz equation

Consider an inhomogeneous medium in $\mathbb{R}^2$ with a compact supported inhomogeneity. The propagation of time-harmonic acoustic waves in the medium obeys the *Helmholtz equation*

$$\Delta u(\mathbf{x}) + k^2 n(\mathbf{x}) u(\mathbf{x}) = 0, \tag{2.1}$$

where $u(\mathbf{x})$ describes the pressure field, $k > 0$ is the wave number and $n(\mathbf{x})$ is the square of the refractive index of the medium, which will be referred as refractive index further. The quantities k and $n(\mathbf{x})$ are related to the frequency ω of the wave and to the speed of propagation in the medium via $k = \omega/c_0$ and $n(\mathbf{x}) = c_0^2/c^2(\mathbf{x})$ where c_0 the speed of the propagation in the homogeneous medium and $c(\mathbf{x})$ is the speed at the point $\mathbf{x} \in \mathbb{R}^2$ (see [Colton1992, Werner1960]).

2.1 Radiation condition

The Helmholtz equation itself does not have a unique solution, which follows from the lemma:

Lemma 2.1.1 *Let $H_0^{(1)}$ and $H_0^{(2)}$ be the Hankel functions of the first and second kind respectively. Then the functions*

$$G(\mathbf{x}, \mathbf{y}) = -\frac{i}{4} H_0^{(1)}(k|\mathbf{x} - \mathbf{y}|), \quad \widetilde{G}(\mathbf{x}, \mathbf{y}) = \frac{i}{4} H_0^{(2)}(k|\mathbf{x} - \mathbf{y}|)$$

are the fundamental solutions of the Helmholtz equation (2.1) with $n(\mathbf{x}) = 1$ in $\mathbb{R}^2$.

Proof See [Vladimirov1971].

The lemma implies that one needs more conditions to guarantee uniqueness. Sommerfeld was first who proposed to consider the behaviour of a solution for the large values of $r = |\mathbf{x}|$ and stated a *radiation condition* to select solutions of physical meaning. He formulated the radiation condition in his paper [Sommerfeld1912] for the tree-dimensional case. Rellich extended the Sommerfeld's radiation condition for the arbitrary-dimensional case [Rellich1943]. For the two-dimensional case, which is of our interest, the radiation condition is

$$\lim_{r\to\infty} \sqrt{r}\left(\frac{\partial u}{\partial r} - iku\right) = 0 \tag{2.2}$$

uniformly in all directions.

More detailed account of the history of this problem can be found in [Miranker1957, Magnus1949].

2.2 Unique solvability of the direct scattering problem

Now we are ready to complete the statement of the problem, prove uniqueness of a solution and then turn to the existence. Since the solvability of the scattering problem requires more regularity from the refractive index than it is required for the uniqueness, we formulate it in the higher regularity assumption on the refractive index. All results from this section are well-known. For this reason we do not give proofs.

2.2.1 The direct scattering problem

The problem describing the scattering of an incident wave $u_i(\mathbf{x})$ in an inhomogeneous medium with a compact inhomogeneity in $\mathbb{R}^2$ can be formulated as follows. Assume that $k > 0$ and $n \in C^{0,\gamma}(\mathbb{R}^2)$, $0 < \gamma < 1$ with $supp(1-n) \subset B(R)$ with $B(R) = \{\mathbf{x} \in \mathbb{R}^2 : |\mathbf{x}| < R\}$ are known and $u_i \in C^2(\mathbb{R}^2)$ with

$$\Delta u_i + k^2 u_i = 0$$

is given. The problem is to find $u_s \in C^2(\mathbb{R}^2)$ such that

$$u = u_i + u_s$$

satisfies the Helmholtz equation (2.1)

$$\Delta u(\mathbf{x}) + k^2 n(\mathbf{x}) u(\mathbf{x}) = 0$$

and u_s satisfies the radiation condition (2.2).

2.2.2 Uniqueness

First we are going to show that the direct scattering problem can not have two different solutions. Further we use the uniqueness to show the existence of the solution.

Lemma 2.2.1 *If $u(\mathbf{x}) \in C^2(\mathbb{R}^2)$ solves in $\mathbb{R}^2$ the Helmholtz equation (2.1) and the radiating condition (2.2), then for $S(R) = \{\mathbf{x} \in \mathbb{R}^2 : |\mathbf{x}| = R\}$*

$$\lim_{R\to\infty} \int_{S(R)} |u|^2 ds = 0.$$

Proof See [Colton1992, Hähner1998].

Lemma 2.2.2 (Rellich's lemma) *Assume $R > 0$ and let $u(\mathbf{x}) \in C^2(\mathbb{R}^2 \setminus B(R))$ be a solution of the Helmholtz equation $\Delta u(\mathbf{x}) + k^2 u(\mathbf{x}) = 0$ for $|\mathbf{x}| > R$, which satisfies*

$$\lim_{r\to\infty} \int_{S(r)} |u(\mathbf{x})|^2 ds = 0$$

and the radiation condition (2.2). Then

$$u(\mathbf{x}) = 0$$

for all $|\mathbf{x}| \in \mathbb{R}^2 \setminus B(R)$.

Proof See [Rellich1943, Miranker1957, Kupradze1934].

Lemma 2.2.3 (unique continuation principle) *If $u \in C_0^2(\mathbb{R}^2)$ satisfies $|\Delta u(\mathbf{x})| \le M|u(\mathbf{x})|$ for all $\mathbf{x} \in \mathbb{R}^2$. Then $u(\mathbf{x}) = 0$ for all $\mathbf{x} \in \mathbb{R}^2$.*

Proof See [Hähner1996].

We combine the lemmas above to prove the following theorem.

Theorem 2.2.4 *The direct scattering problem (2.2.1) has at most one solution.*

Proof Since the problem (2.2.1) is linear it is enough to prove that the problem with null incident field has only trivial solution. For the homogeneous Helmholtz equation we obviously have

$$|\Delta u(\mathbf{x})| = |k^2 n(\mathbf{x}) u(\mathbf{x})| \le M|u(\mathbf{x})|, \quad M = \max_{x\in\mathbb{R}^2} |k^2 n(\mathbf{x})|.$$

Moreover, by Rellich's lemma $supp(u) \subset\subset \mathbb{R}^2$. Thus, $u(\mathbf{x}) = 0$ for all $\mathbf{x} \in \mathbb{R}^2$. □

Remark 2.2.5 *The uniqueness result remains in the case of $n(\mathbf{x}) \in L^2(\mathbb{R}^2)$ [Hähner1998].*

2.2.3 Existence of the solution

Now we are going to show the solvability of the problem (2.2.1).

First we give a representation of smooth functions in a bounded domain with a smooth boundary in terms of fundamental solutions.

Lemma 2.2.6 (Green's representation formula) *Let $\Omega \subset \mathbb{R}^2$ be a nonempty bounded domain with C^2-smooth boundary and let $G(\mathbf{x}, \mathbf{y})$ be the fundamental solution of the Helmholtz equation satisfying the radiating condition. Then for a function $u \in C^2(\overline{\Omega})$ the following representation formula holds for $\mathbf{x} \in \Omega$*

$$u(\mathbf{x}) = \int\limits_{\partial\Omega} \left(\frac{\partial u}{\partial \nu(\mathbf{y})} G(\mathbf{x}, \mathbf{y}) - u(\mathbf{y}) \frac{\partial G}{\partial \nu(\mathbf{y})}(\mathbf{x}, \mathbf{y}) \right) ds(\mathbf{y}) - \int\limits_{\Omega} (\Delta u(\mathbf{y}) + k^2 u(\mathbf{y})) G(\mathbf{x}, \mathbf{y}) d\mathbf{y},$$

where $\nu(\mathbf{y})$ denotes the unit exterior normal to the $\partial\Omega$ at $\mathbf{y}$.

Proof See [Colton1992].

Remark 2.2.7 *Green's formula is also true in the case of $u \in C^2(\Omega) \bigcap C^1(\overline{\Omega})$ with $\Delta u + k^2 u \in C(\overline{\Omega})$ [Colton1992].*

Applying the Green's representation formula (2.2.6) to the solution u of the problem (2.2.1) for $\Omega = B(r)$ and $r > |\mathbf{x}| + R$ we arrive at the equation

$$u(\mathbf{x}) = \int\limits_{\partial B(r)} \left(\frac{\partial u}{\partial \nu(\mathbf{y})} G(\mathbf{x}, \mathbf{y}) - u(\mathbf{y}) \frac{\partial G(\mathbf{x}, \mathbf{y})}{\partial \nu(\mathbf{y})} \right) ds(\mathbf{y}) - k^2 \int\limits_{B(r)} (1 - n(\mathbf{y})) u(\mathbf{y}) G(\mathbf{x}, \mathbf{y}) d\mathbf{y}.$$

Putting $u = u_i + u_s$ in the first integral we obtain the *Lippmann-Schwinger* equation

$$u(\mathbf{x}) = u_i(\mathbf{x}) - k^2 \int\limits_{B(R)} (1 - n(\mathbf{y})) u(\mathbf{y}) G(\mathbf{x}, \mathbf{y}) d\mathbf{y}, \quad \mathbf{x} \in \mathbb{R}^2,$$

which is the integral equation in $B(R)$ for the unknown field u. Using the Lippmann-Schwinger equation we can prove that the direct scattering problem has a solution.

Lemma 2.2.8 *Let $u \in C(\overline{B(R)})$ be a solution of the Lippman-Schwinger equation in $B(R)$. Define $u_s(\mathbf{x})$ by*

$$u_s(\mathbf{x}) = -k^2 \int_{B(R)} (1 - n(\mathbf{y}))u(\mathbf{y})G(\mathbf{x}, \mathbf{y})d\mathbf{y}, \quad \mathbf{x} \in \mathbb{R}^2,$$

then u_s is a solution of the direct scattering problem (2.2.1).

Proof See [Colton1992].

Lemma 2.2.9 *The Lippmann-Schwinger equation (2.2.3) is a Fredholm integral equation of the second kind with a compact integral operator in $C(\overline{B(R)})$*

Proof See [Colton1992].

Theorem 2.2.10 *The direct scattering problem (2.2.1) has a solution.*

Proof The Lippman-Schwinger equation, being the Fredholm integral equation of the second kind, has a unique solution, if it has a trivial nullspace. Since the solution of the direct scattering problem is unique the nullspace is trivial. Since the solution of the Lippman-Schwinger equation yields a solution of the scattering problem (2.2.1), the problem (2.2.1) has a solution. □

2.3 Examples

In only few cases the Helmholtz equation (2.1) has an analytical solution. We discuss here some cases which will be used in the next sections.

Before we start with cases of nonconstant refractive index, we notice that in the case of a homogeneous medium, i.e., for $n(\mathbf{x}) = 1$, the direct scattering problem has a trivial solution $u_s = 0$. Thus, the whole wave field is $u = u_i + u_s = u_i$, where u_i is a plane wave moving in the direction $\Theta = (\cos(\theta), \sin(\theta))$ with $0 \leq \theta < 2\pi$

$$u_i(\mathbf{x}) = \exp(ik\mathbf{x} \cdot \Theta).$$

Unless otherwise stipulated we will use only plane incident waves.

2.3.1 Scattering on a homogeneous disk

The first case is the scattering on a homogeneous disk. We consider the disk of radius R with the centrum at the origin and refractive index is equal to n inside of the disk, i. e. the Helmholtz equation with the refractive index $n(\mathbf{x})$ is

$$n(\mathbf{x}) = \begin{cases} n, \text{ for } |\mathbf{x}| \leq R \\ 1, \text{ for } |\mathbf{x}| > R \end{cases} \tag{2.3}$$

Theorem 2.3.1 *The Helmholtz equation (2.1) with the refractive index (2.3) together with the radiation condition (2.2) for the scattered part u_s has the solution*

$$u(r, \varphi) = \sum_{q=-\infty}^{\infty} i^q \exp(iq\varphi) a_q J_q(k_1 r) \tag{2.4}$$

for $r < R$ and $k_1 = k\sqrt{n}$ and

$$u(r, \varphi) = \sum_{q=-\infty}^{\infty} i^q \exp(iq\varphi)(J_q(kr) + b_q H_q(kr)) \tag{2.5}$$

for $r > R$, where (r, φ) are the polar coordinates of $\mathbf{x} \in \mathbb{R}^2$ and the coefficients a_q and b_q do not depend on (r, φ).

Proof First we treat the Helmholtz equation with a constant wave number k in polar coordinates (r, φ)

$$\frac{1}{r}\frac{\partial}{\partial r}\left(r\frac{\partial u}{\partial r}\right) + \frac{1}{r^2}\frac{\partial^2 u}{\partial \varphi^2} + k^2 u = 0. \tag{2.6}$$

Separating the variables

$$u(r,\varphi) = u_r(r)u_\varphi(\varphi)$$

we arrive at the equation

$$\frac{1}{r}u_\varphi\left(r\frac{d^2u_r}{dr^2} + \frac{du_r}{dr}\right) + \frac{1}{r^2}u_r\frac{d^2u_\varphi}{d\varphi^2} + k^2u_ru_\varphi = 0.$$

Hence the function $u_\varphi(\varphi)$ satisfies differential equation

$$u_\varphi'' + q^2u_\varphi = 0$$

for some constant q, therefore the function $u_r(r)$ satisfies Bessel equation

$$u_r'' + \frac{1}{r}u_r' - \left(k^2 - \frac{q^2}{r^2}\right)u_r = 0.$$

The first differential equation has two linear independent solutions

$$u_\varphi(\varphi) = \left\{ \begin{array}{l} \exp(iq\varphi) \\ \exp(-iq\varphi) \end{array} \right\}$$

and the second equation

$$u_r(r) = \left\{ \begin{array}{l} J_q(kr) \\ H_q(kr) \end{array} \right\}$$

where $k \neq 0$, $q \in \mathbb{N}$, $J_q(z)$ and $H_q(z)$ are Bessel and Hankel functions respectively.

Thus, functions

$$u_q(r,\varphi) = \left\{ \begin{array}{l} J_q(kr) \\ H_q(kr) \end{array} \right\} \cdot \left\{ \begin{array}{l} e^{iq\varphi} \\ e^{-iq\varphi} \end{array} \right\} \tag{2.7}$$

solve the Helmholtz equation (2.6) for every q.

See [Abramowitz1965] for the proofs of the following lemmas.

Lemma 2.3.2 *The functions $J_q(z)$ and $H_q(z)$ form a fundamental system of solutions of the Bessel's differential equation.*

Lemma 2.3.3 *The functions $H_q(kr)\exp(iq\varphi)$ satisfy the radiation condition (2.2).*

Moreover, the plane wave can be presented in terms of the Bessel functions $J_q(z)$. It is a direct consequence of the lemma [Smirnov1972]:

Lemma 2.3.4 *The function* $\exp(z(t-1/t)/2)$ *is the generating function for the Bessel functions with integer index, that is,*

$$\exp\left(\frac{1}{2}z(t-\frac{1}{t})\right) = \sum_{q=-\infty}^{+\infty} J_q(z)t^q.$$

Thus, the plane wave $\exp(ikr\cos(\varphi))$ has the representation in terms of the Bessel functions

$$\exp(ikr\cos(\varphi)) = \sum_{q=-\infty}^{+\infty} i^q J_q(kr)\exp(iq\varphi),$$

where the series converges uniformly on every compact set.

Now we return to the problem of scattering of a plane wave on a homogeneous disk. The function $u(r,\varphi)$ defined in (2.4, 2.5) satisfies the Helmholtz equation

$$\Delta u + k_1^2 u = 0$$

inside $B(R)$ and the Helmholtz equation

$$\Delta u + k^2 u = 0$$

outside $B(R)$. Further, the scattered part $u_s(r,\varphi)$ of the solution $u(r,\varphi)$

$$u_s(r,\varphi) = \sum_{q=-\infty}^{+\infty} i^q \exp(iq\varphi) b_q H_q(kr),$$

satisfies the radiation condition. We choose the coefficients a_q and b_q so that the whole function $u(r,\varphi)$ and its normal derivative $\partial u(r,\varphi)/\partial\nu$ are continuous on the boundary of the disk. It means that the system of equations

$$\begin{aligned} a_q J_q(k_1 R) &= J_q(kR) + b_q H_q(kR) \\ a_q J_q'(k_1 R) &= J_q'(kR) + b_q H_q'(kR) \end{aligned} \tag{2.8}$$

has to be hold. Since Bessel functions of any kind with an integer index fulfill the condition [Abramowitz1965]

$$\mathcal{C}_{q-1}(z) - \mathcal{C}_{q+1}(z) = 2\mathcal{C}_q'(z),$$

the last equation of the system (2.8) can be written as

$$\begin{aligned} &a_q k_1 (J_{q-1}(k_1 R) - J_{q+1}(k_1 R)) = \\ &k(J_{q-1}(kR) - J_{q+1}(kR)) + b_q k(H_{q-1}(kR) - H_{q+1}(kR)). \end{aligned} \tag{2.9}$$

Thus, we have the system of linear equations to define a_q and b_q. The case $a_q = 0$ is trivial, otherwise we have a linear system to define $1/a_q$ and b_q/a_q. This system has the determinant

$$det = H_q(kR)J'_q(kR) - H'_q(kR)J_q(kR),$$

which is the Wronski-determinant of the functions $H_q(kR)$ and $J_q(kR)$. $det \neq 0$ for $kR > 0$ [Abramowitz1965]. $\square$

The next figures show the incident wave field u_i, the solution of the Helmholtz equation (2.4,2.5) u and the scattered part u_s for different values of k. For the numerical details see [Wübbeling1994].

We see that the scattered field u_s is much smaller than the incident field u_i. Moreover, in the case of a large value of k the whole wave field u becomes stronger after passing the circle. We will see further that the geometrical-optics approximation is not valid in the neighbourhood of this area.

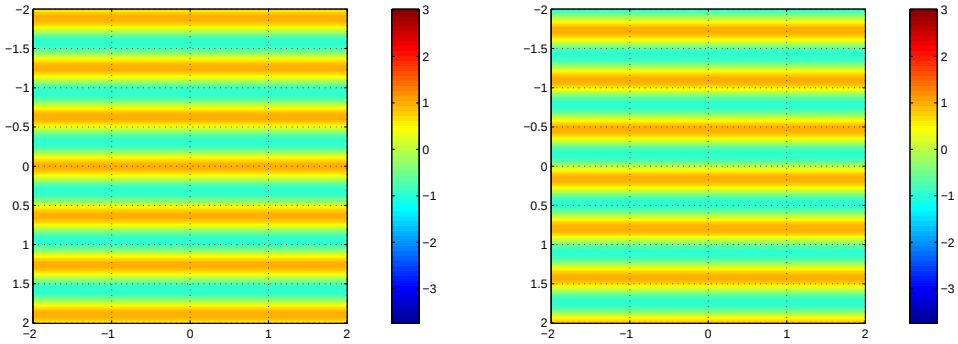

Figure 2.1: The real (left) and imaginary (right) parts of the incident wave u_i for $k = 10$ and the side of the square $Side = 4$.

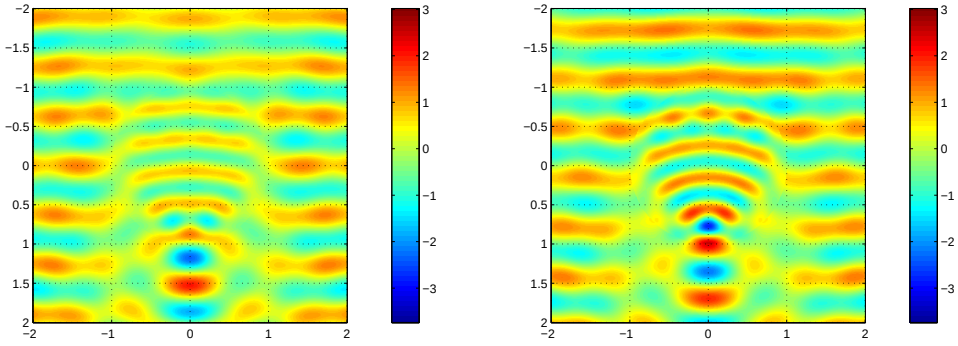

Figure 2.2: The real (left) and imaginary (right) parts of the resulting field u for $k = 10$, $n = 1.37$, the disk radius $R = 1$, the square side $Side = 4$.

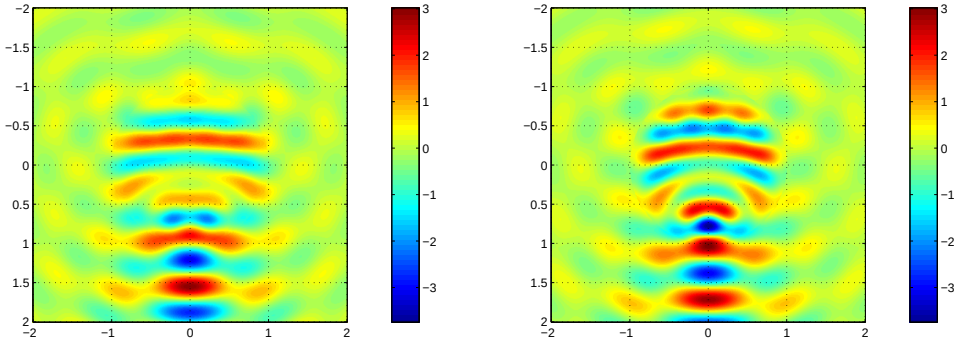

Figure 2.3: The real (left) and imaginary (right) parts of the scattered field u_s for $k = 10$, $n = 1.37$, the disk radius $R = 1$, the square side $Side = 4$.

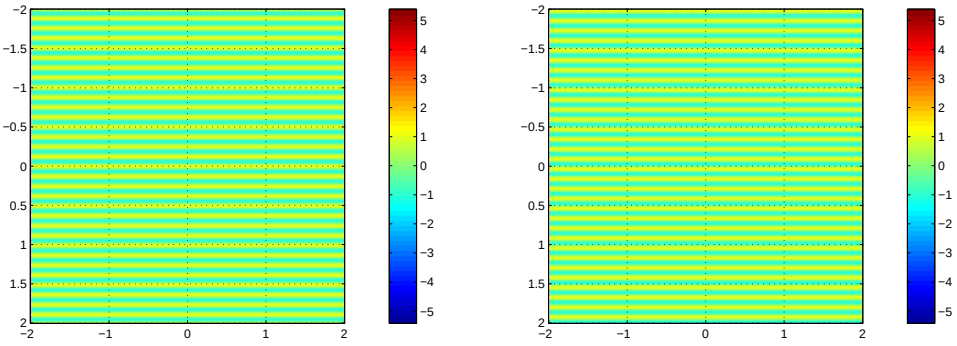

Figure 2.4: The real (left) and imaginary (right) parts of the incident wave u_i for $k = 50$ and the side of the square $Side = 4$.

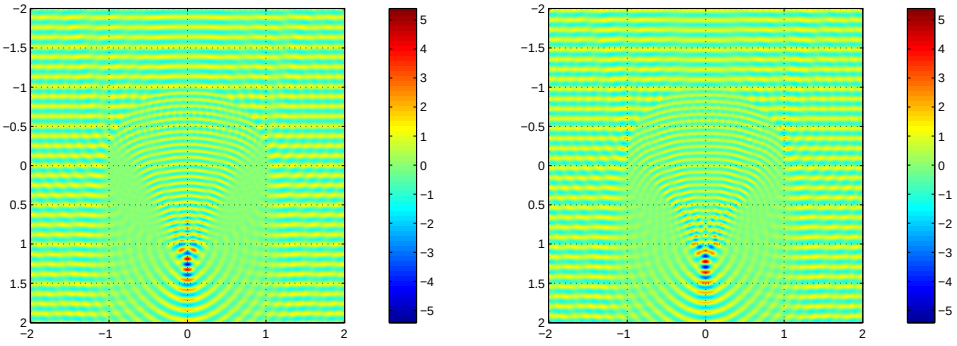

Figure 2.5: The real (left) and imaginary (right) parts of the resulting field u for $k = 50$, $n = 1.37$, the disk radius $R = 1$, the square side $Side = 4$.

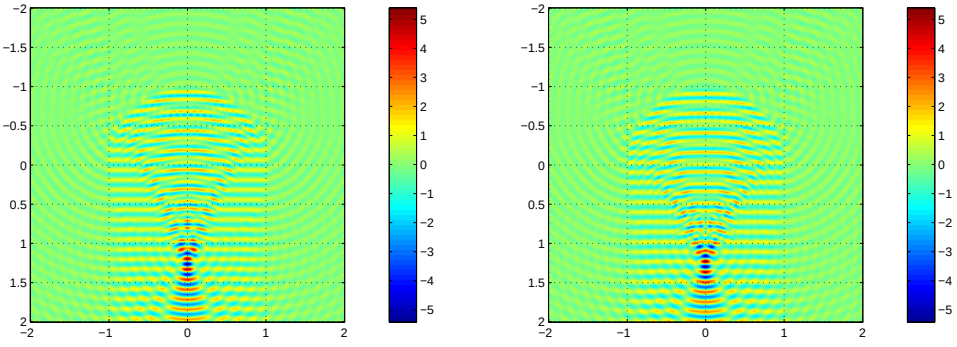

Figure 2.6: The real (left) and imaginary (right) parts of the scattered field u_s for $k = 50$, $n = 1.37$, the disk radius $R = 1$, the square side $Side = 4$.

2.3.2 Scattering on two concentric disks

Similarly to the problem considered in the previous section the scattering on the homogeneous disk the problem of the scattering of a plane wave on a homogeneous ring and a concentric disk in it can be treated. In this case we look for the solution of the Helmholtz equation with the refractive index

$$n(\mathbf{x}) = \begin{cases} n_1, \text{ for } |\mathbf{x}| \leq R_1 \\ n_2, \text{ for } R_1 \leq |\mathbf{x}| \leq R_2 \\ 1, \text{ for } |\mathbf{x}| > R_2 \end{cases}$$

where $R_1 < R_2$ are the radii of the smaller and larger disks respectively.

The solution in polar coordinates (r, φ) is supposed to have the form

$$u(r, \varphi) = \sum_{q=-\infty}^{\infty} i^q \exp(iq\varphi) a_q J_q(k_1 r) \tag{2.10}$$

for $r < R$ and with $k_1 = k\sqrt{n_1}$

$$u(r, \varphi) = \sum_{q=-\infty}^{\infty} i^q \exp(iq\varphi)(b_q J_q(k_2 r) + c_q H_q(k_2 r)) \tag{2.11}$$

for $R_1 < r < R_2$ and $k_2 = k\sqrt{n_2}$ and

$$u(r, \varphi) = \sum_{q=-\infty}^{\infty} i^q \exp(iq\varphi)(J_q(kr) + d_q H_q(kr)) \tag{2.12}$$

for $r > R_2$. Again choosing the coefficients a_q, b_q, c_q and d_q to obtain the $C^2(\mathbb{R}^2)$ function $u(r, \varphi)$ we derive a system of linear equations for the coefficients.

The following figures show again the incident wave field u_i, the solution of the Helmholtz equation u and the scattered part u_s of it for the square with the side $Side = 4$ and the radii of disks $R_1 = 0.5$, $R_2 = 1$, $k = 50$, $n_1 = 1.2$ $n_2 = 1.1$ (the values of the wave numbers are $k_1 = 60$ and $k_2 = 55$ in this case). Further we will use this exact solution to test our reconstruction method.

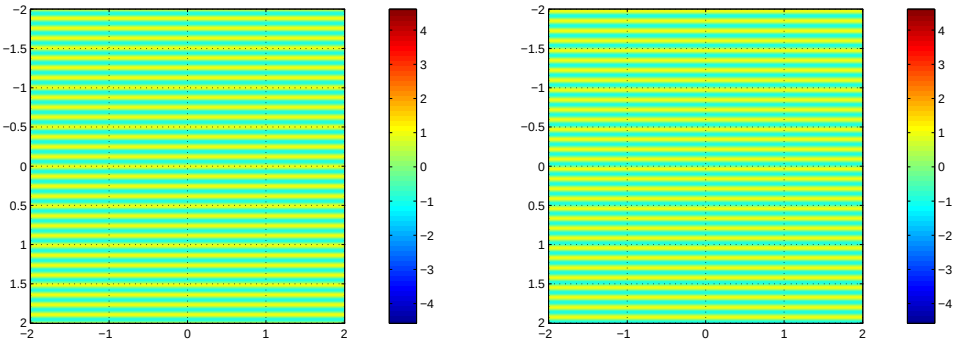

Figure 2.7: The real (left) and imaginary (right) parts of the incident wave u_i for $k = 50$ and the side of the square $Side = 4$.

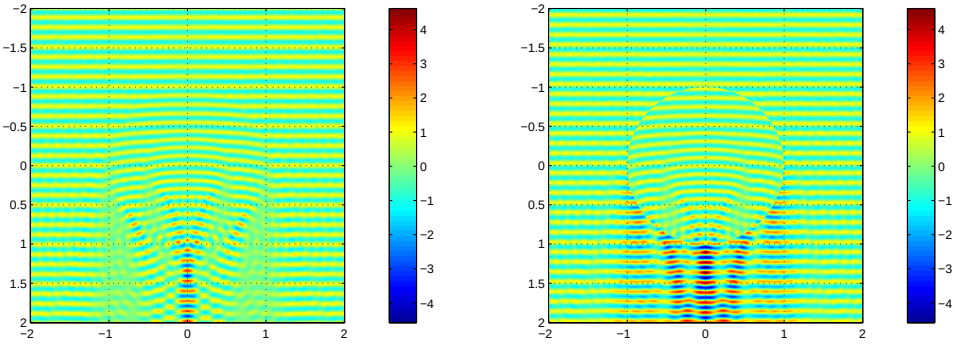

Figure 2.8: The real (left) and imaginary (right) parts of the resulting field u for $k = 50$, radii of disks $R_1 = 0.5$, $R_2 = 1$, $n_1 = 1.2$, $n_2 = 1.1$.

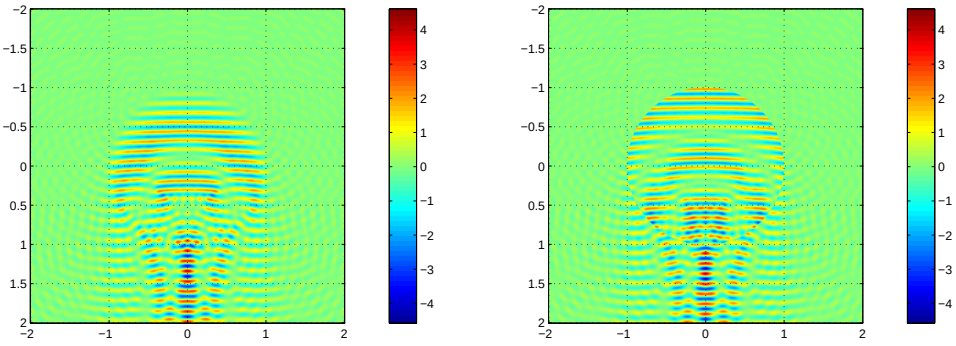

Figure 2.9: The real (left) and imaginary (right) parts of the scattered field u_s for $k = 50$, radii of disks $R_1 = 0.5$, $R_2 = 1$, $n_1 = 1.2$, $n_2 = 1.1$.

Chapter 3

The eikonal approximation

3.1 The asymptotic expansion

In the case of an arbitrary smooth refractive index $n(\mathbf{x})$ the analytical solution of the Helmholtz equation usually does not exist. But we still want to study the behaviour of the solution in the high-frequent case. That is, we are interested in the finding of some approximation for the solution of the Helmholtz equation (2.1)

$$\Delta u(\mathbf{x}, k) + k^2 n(\mathbf{x}) u(\mathbf{x}, k) = 0$$

with a smooth variable nonnegative refractive index $n(\mathbf{x})$ for large values of k.

We suppose that the equation has only one solution, i.e, we require the sufficient smoothness for the refractive index and the radiation condition (2.2) for the scattered part $u_s = u - u_i$ of the wave field u.

The usual way to describe high-frequent wave fields is to obtain an *asymptotic expansion* and to study it.

Definition 3.1.1 *The sequence of functions $a_j(\varepsilon)$, $j \in \mathbb{N}_0$ is called an asymptotic sequence as $\varepsilon \to 0$ if*

$$a_{j+1}(\varepsilon) = o(a_j(\varepsilon)), \quad as \quad \varepsilon \to 0.$$

Given a function $g(\mathbf{x}, \varepsilon)$, we call the series $\sum_{j=0}^{N} g_j(\mathbf{x}) a_j(\varepsilon)$ an asymptotic expansion for the function g

$$g(\mathbf{x}, \varepsilon) \sim \sum_{j=0}^{N} g_j(\mathbf{x}) a_j(\varepsilon) \quad as \quad \varepsilon \to 0$$

where the coefficients $g_j(\mathbf{x})$ *are the functions of* $\mathbf{x}$ *only and* $a_j(\varepsilon)$ *is the asymptotic sequence, if*

$$g(\mathbf{x},\varepsilon) = \sum_{j=0}^{N-1} g_j(\mathbf{x}) a_j(\varepsilon) + r_N(\mathbf{x},\varepsilon),$$

$$r_N(\mathbf{x},\varepsilon) = O(a_N(\varepsilon)).$$

Lemma 3.1.1 *The functions* $g_j(\mathbf{x})$ *can be determined uniquely from the members of the asymptotic sequence.*

Proof See [Nayfeh1973].

The asymptotic series, which is used to describe the wave field $u = u_i + u_s$ is called the *geometrical-optics approximation* or the *ray series*. We are looking for the solution in the form of the asymptotic series in terms of the small parameter $1/k$

$$u(\mathbf{x},k) \sim \exp(ik\phi(\mathbf{x})) \sum_{j=0}^{\infty} \frac{1}{(ik)^j} u_j(\mathbf{x}) \tag{3.1}$$

where functions $\phi(\mathbf{x}), u_j(\mathbf{x})$ are to be determined.

3.2 The eikonal approximation

Substituting the ray series (3.1) into the equation (2.1) and separating powers of k we arrive at the equations :

$$|\nabla\phi(\mathbf{x})|^2 - n(\mathbf{x}) = 0 \tag{3.2}$$

for $\phi(\mathbf{x})$ and

$$2\nabla\phi\nabla u_j + u_j\Delta\phi - \Delta u_{j-1} = 0 \tag{3.3}$$

for $u_j(\mathbf{x})$ with

$$j \in \mathbb{N}_0; \quad u_{-1} = 0.$$

The equation (3.2) is called the *eikonal equation* and its solution ϕ *eikonal function* or *eikonal*. The equations (3.3) are called the *transport equations*.

Remark 3.2.1 *The notion* ***eikonal*** *(from the Greek* $\varepsilon\iota\kappa\omega\nu$ *means* ***image****) was introduced first by H.Bruns in 1895 [Bruns1895].*

Further we will use only the first two terms of the ray series to approximate the solution of the Helmholtz equation (2.1).

Definition 3.2.1 *The expression provided by the first term of the ray series*

$$u_E(\mathbf{x}) = A(\mathbf{x}) \exp(ik\phi(\mathbf{x})) \tag{3.4}$$

is called the eikonal approximation of the solution $u(\mathbf{x})$.

3.3 The eikonal equation and rays

The eikonal equation in some way contains all of geometrical optics within itself. Solving it we come to the basic objects of geometrical optics.

To solve the eikonal equation we consider the Fermat functional

$$\Phi(\gamma) = \int_{\mathbf{x}_0}^{\mathbf{x}} \sqrt{n(\gamma(s))} ds, \tag{3.5}$$

where $\mathbf{x}_0$ and $\mathbf{x}$ are points in $\mathbb{R}^2$, γ is a curve joining them with $|\gamma'(s)| = 1$, and ds is an arc length element. This functional represents the time required for a wave disturbance propagating with the velocity $c(\mathbf{x}) = c_0/\sqrt{n}(\mathbf{x})$ to travel between two points $\mathbf{x}_0$ and $\mathbf{x}$ along the curve γ.

Definition 3.3.1 *The curve* γ *is called an extremal curve or characteristic of the functional (3.5) if it satisfies the Euler equation*

$$\frac{d}{ds}(\mathbf{s}_0\sqrt{n}) - \nabla\sqrt{n} = 0, \tag{3.6}$$

where $\mathbf{s}_0$ *is a unit vector tangent to* γ.

Definition 3.3.2 (Fermat's principle) *The extremal curves of the Fermat's functional are called rays.*

The Fermat's principle can be used to derive the Snell's law of geometrical optic, which describes the refraction of a ray path at an interface between media of different refractive indexes: n_1, the refracting index of the "medium of incidence", and n_2, the refracting index of the "medium of refraction".Let θ_1 and θ_2 be the angels which the incident and the refracted rays make with the normal to the refracting surface.

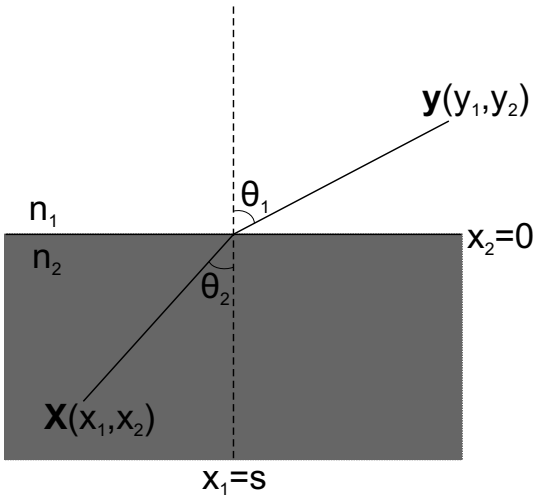

Figure 3.1: refraction of a ray by Snell's law, $n_2 > n_1$.

The total time between points $\mathbf{x}$ and $\mathbf{y}$ is

$$\phi = n_2\sqrt{x_2^2 + (s - x_1)^2} + n_1\sqrt{y_2^2 + (s - y_1)^2}$$

and by Fermat's principle $d\phi/ds = 0$, so

$$\frac{n_2(s - x_1)}{\sqrt{x_2^2 + (s - x_1)^2}} + \frac{n_1(s - y_1)}{\sqrt{y_2^2 + (s - y_1)^2}} = 0,$$

which gives the Snell's law

$$n_2 \sin(\theta_2) = n_1 \sin(\theta_1). \tag{3.7}$$

We will use the Snell's law to test some numerical examples.

Let us return to the eikonal equation. Consider the function

$$\phi(\mathbf{x}, \mathbf{x}_0) = \int_{\mathbf{x}_0}^{\mathbf{x}} \sqrt{n} ds, \tag{3.8}$$

where the integral is taken along the extremal curve.

Lemma 3.3.1 *The function ϕ satisfies the eikonal equation (3.2), that is,*

$$|\nabla \phi|^2 = n.$$

Proof See [Babich1991, Babich1979].

The common way to find the extremal curves of the functional (3.5) is based on incorporating of the associated Hamiltonian system (see [Hörmander1994]). Let $H(\mathbf{x}, \mathbf{p})$ be the Hamiltonian function of a form

$$H(\mathbf{x}, \mathbf{p}) = \frac{1}{2}(|\mathbf{p}|^2 - n(\mathbf{x})),$$

which corresponds to the Helmholtz equation (2.1). Here $\mathbf{p}$ is the momentum of the extremal curve, which indicates the direction of the propagation $\mathbf{p}/|\mathbf{p}|$. The corresponding Hamiltonian equations are

$$\begin{aligned} \dot{\mathbf{x}} &= \nabla_p H(\mathbf{x}, \mathbf{p}) = \mathbf{p} \\ \dot{\mathbf{p}} &= -\nabla_x H(\mathbf{x}, \mathbf{p}) = \nabla n(\mathbf{x})/2, \end{aligned} \tag{3.9}$$

where an appropriate initial condition

$$(\mathbf{x}^0(t), \mathbf{p}^0(t)) \tag{3.10}$$

is assumed for $\mathbf{x}(s), \mathbf{p}(s)$ at $s = 0$. The extremal curves are solutions $\mathbf{x}(s)$.

Definition 3.3.3 *The trajectories* $(\mathbf{x}(t, s), \mathbf{p}(t, s))$*, which solve the initial value problem (3.9,3.10) are called bicharacteristics.*

Lemma 3.3.2 *Along the bicharacteristics holds* $|p(s)|^2 = n(x(s))$.

Proof See [Kucherenko1969].

3.4 Ray coordinates and the transport equation

With the help of rays we have found the eikonal function ϕ. To complete the eikonal approximation (3.4) we will find the function $A(\mathbf{x})$ representing the amplitude of the wave field, that is, we are going to solve the transport equation (3.3). To solve this equation we consider a new coordinate system which is naturally connected with rays and *wave fronts*, surfaces with a constant value of the eikonal ϕ. We take a wave front S with some fixed value of $\phi = \phi_0$ on it. Let α be a parameter defining a point on S. Through each point $\mathbf{x}_0 \in S$ we pass a ray perpendicular to S at this point. A point on the ray we characterize then by the value of the eikonal according to (3.8).

Thus, in the neighborhood of the wave front S the coordinate system (α, ϕ) is defined : α defines the point $\mathbf{x}_0$ on S and at a point $\mathbf{x}$ on the ray γ

$$\phi(\mathbf{x}, \mathbf{x}_0) = \phi_0 \pm \int_{\mathbf{x}_0}^{\mathbf{x}} \sqrt{n(\gamma(s))} ds,$$

with $\phi_0 = \text{const}$. The "+" sign should be taken on one side of S and the "-" sign on the other.

Remark 3.4.1 *Often we will use the notation $\phi(\mathbf{x})$. We mean that giving the initial wave front we consider a ray $\gamma_x(s)$ starting on the wave front and ending at the point $\mathbf{x}$: $\gamma_x(s_x) = \mathbf{x}$ and calculate the value of the eikonal over this ray starting on the given wave front:*

$$\phi(\mathbf{x}) = \int_0^{s_x} \sqrt{n(\gamma_x(s))} ds. \tag{3.11}$$

Definition 3.4.1 *The coordinates α, ϕ are called ray coordinates.*

The transport equation (3.3) for $j = 0$

$$2\nabla\phi\nabla u_0 + u_0 \Delta\phi = 0 \tag{3.12}$$

is easily solvable in terms of the ray coordinates. First we rewrite this equation.

Lemma 3.4.2

$$2\nabla\phi\nabla u_0 = 2\frac{\nabla\phi}{|\nabla\phi|}\nabla u_0 |\nabla\phi| = 2n\frac{\partial u_0}{\partial\phi}$$

and

$$\Delta\phi = \frac{n}{J}\frac{\partial J}{\partial\phi},$$

where for a point $\mathbf{x} = (x_1, x_2)$

$$J = \frac{\partial(x_1, x_2)}{\partial(\alpha, \phi)} \tag{3.13}$$

is the Jacobian of the transformation from the cartesian to the ray coordinates.

Proof See [Babich1991, Babich1979].

Hence the transport equation (3.12) can be rewritten as

$$2n\frac{\partial A}{\partial \phi} + A\frac{n}{J}\frac{\partial J}{\partial \phi} = 0.$$

The solution of this equation is

$$A = a_0\sqrt{\frac{1}{J}}, \tag{3.14}$$

where a_0 is a constant along each ray.

Now we have solved both the eikonal and transport equations. Thus, given the initial wave front Γ with $\phi|_\Gamma = 0$ and supposing that the initial $a_0 = 1$ (which is true for the case of the initial plane wave) we have found for the eikonal approximation:

$$u_E(\mathbf{x}) = \sqrt{\frac{1}{J}}\exp\left(ik\int_0^{s_0}\sqrt{n(\gamma(s))}ds\right).$$

Here the ray γ satisfies $\gamma(s_0) = \mathbf{x}$.

3.5 Examples of a ray tracing

Ray tracing is a wide used numerical technique to characterize the wave propagation. It consists in solving of the Hamiltonian system, which describes bicharacteristics and, therefore, rays. With the help of ray tracing the propagation is reduced to the set of independent initial-value problems, each of them defines a single ray.

In this section we are going to show ray tracing examples in media with various profiles $n(\mathbf{x})$.

3.5.1 Scattering on a homogeneous disk

We start with scattering on a homogeneous disk of radius $\rho = 1$ with refractive index $n = \text{const}$, i.e.

$$n(\mathbf{x}) = \begin{cases} n, \text{ for } |\mathbf{x}| \leq \rho \\ 1, \text{ for } |\mathbf{x}| > \rho \end{cases} . \tag{3.15}$$

We apply the Snell's law (3.7) to the problem of scattering on a homogeneous disk to calculate the rays traces exactly. This exact solution coincides with the numerical one, calculated by use of the Hamiltonian system (3.9) for $n(\mathbf{x})$ smoothed by use of Fourier series.

The next figures show the ray tracing for the Snell's index $n_{Snell} = n_{outside}/n_{inside} = 0.65$, which corresponds to $n = 2.37$.

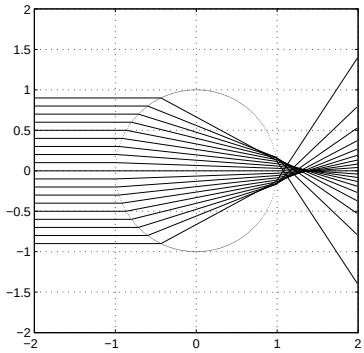

Figure 3.2: rays calculated by use of Snell's law.

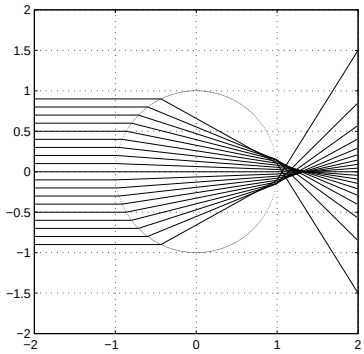

Figure 3.3: rays calculated using the Hamiltonian system.

3.5.2 Luneberg Lens

The next example is the propagation through a medium with index of refraction which varies with distance r from the centrum of some sphere. The classical Luneberg lens [Luneberg1944] has a value of one at the surface of the sphere and two at its centrum. The refractive index of this lens is given by

$$n(r) = \begin{cases} 2 - \left(\frac{r}{R}\right)^2 & \text{for} \quad r < R, \\ 1, \quad \text{otherwise}, \end{cases} \tag{3.16}$$

where R is a radius of the lens. It is presented in the following figure.

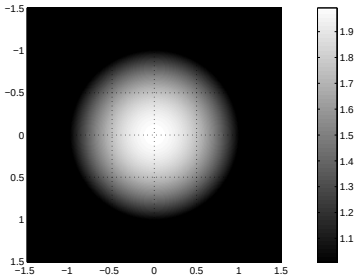

Figure 3.4: the refractive index: $n(r) = 2 - r^2$.

It is known [Morgan1958], that the Luneberg lens focuses a parallel rays bundle to the point on its boundary. For this reason this example is a good test for the numerical calculations of the ray pathes.The refraction of a horizontal plane wave described by the Hamiltonian system, produces the ray family shown on the (Fig. 3.5).

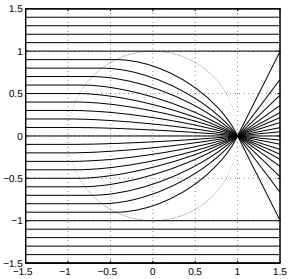

Figure 3.5: parallel rays bundle refracted on the the Luneberg lens (the circle) $n(r) = 2 - r^2$.

3.5.3 Simulated data

For the last two examples we are using data simulating some real velocity or refractive index profiles. The first one represents a slow varying refractive index, while the second one represents a refractive index with strong horizontal and vertical gradients. These two type of data are conditioned by the nature of the problems under consideration.

Figure 3.6 shows a model of a human breast simulated by [Borup1992]. The refractive index is complex. We considered the real part only. With the speed of sound c in the breast tissue, $c_0 = 1500$ m/s the sound speed in the surrounding water we have for the refractive index $n(\mathbf{x}) = 1 + c_0^2/c^2(\mathbf{x})$. The values of c vary in the range from 1458 m/s to 1568 m/s.

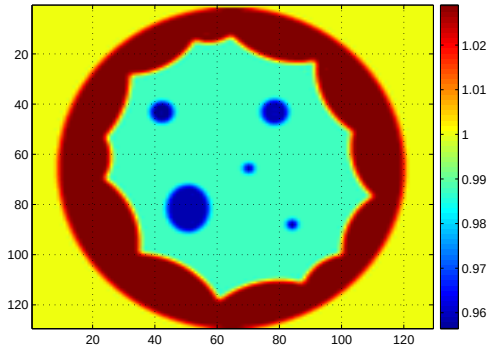

Figure 3.6: the refractive index profile.

The next Figure 3.7 shows the result of the ray tracing for the horizontal incident plane wave.

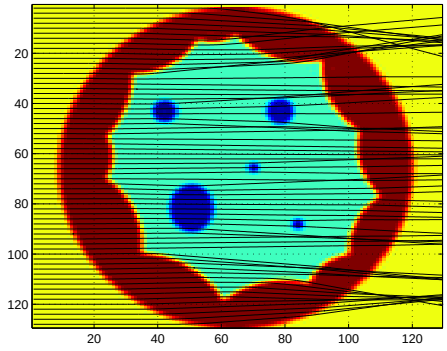

Figure 3.7: ray tracing with the refractive index.

The second example is the Marmousi velocity model. This synthetic data set is based on a profile through the North Quenguela through in the Cuanza basin [Versteeg1993]. It was created to produce a complex seismic data which require advanced processing techniques to obtain a correct earth image. For the ray tracing computation we used the smooth Marmousi model from [Benamou]. The modeled section is 9192 m long and 2904 m deep. The velocity varies between 1500 m/s and 5500 m/s.

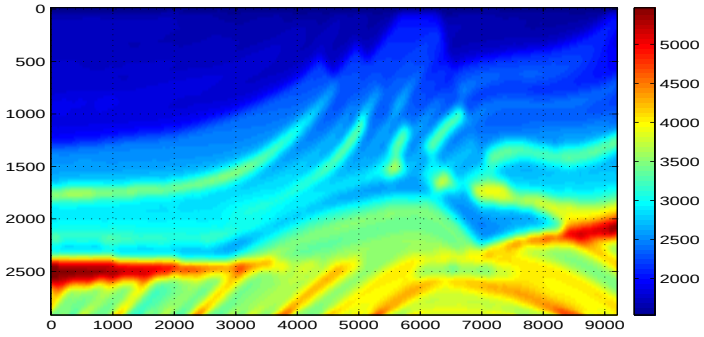

Figure 3.8: The smooth velocity model.

We show the rays tracing calculated by using Hamiltonian system with the point source located at $(6000m, 2800m)$ for the Marmousi model with the velocity normalized by $c_0 = 5500$ m/s.

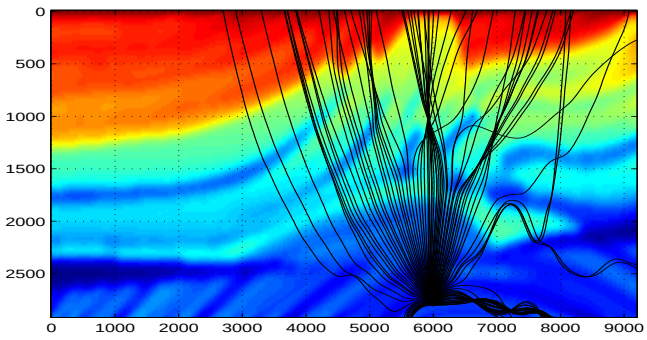

Figure 3.9: Refractive index with the ray tracing for the point source located at $(6000, 2800)$ and rays with starting directions from 0^0 to 180^0 with equal spacing between them.

3.5.4 Some remarks

We are now in a position to discuss our examples. It is clear that even a very simple and smooth refractive index can lead to a singular behavior of the ray family, i.e., to the intersection or focusing of the rays, formation of an envelope of the ray family. That is, eikonal can be a multivalued function. The simulated data profiles show that the picture of the ray tracing for the practical applications is rather complicated and tends to have singularities.

Such a singular behavior is considered in the next section.

3.6 Caustics

Let us return to the eikonal approximation (3.4). As it can be seen from the expression

$$u_E(\mathbf{x}) = \frac{1}{\sqrt{J(\mathbf{x})}} \exp(ik\phi(\mathbf{x})),$$

the eikonal approximation breaks down whenever $J = 0$, where J is the *geometrical divergence*, the Jacobian of the transformation from the cartesian to ray coordinates. Although $J \neq 0$ for the initial field, it does not necessarily remain nonzero and the amplitude calculated by the expression (3.14) blows up at these points.

Definition 3.6.1 *The set* $\{\mathbf{x} : J(\mathbf{x}) = 0\}$ *is called caustic.*

So the ray structure breaks down in the neighborhood of a caustic, because the ray family cannot be uniquely resolved for the ray coordinates. Since the amplitude becomes infinite at a caustic, the eikonal approximation is not valid any more as it is known that the solutions of the Helmholtz equation are analytic outside the support of singular sources in a case of a smooth index of refraction [Gilbarg2001]. However, exact solutions which are available for some cases (see, e.g., section (2.3.1)), show that the wave field becomes very strong in the neighborhood of a caustic.

To describe wave fields in the neighbourhood of caustics local and uniform methods were investigated. The first type of methods is based on the *boundary layer* techniques (see [Babich1979, Babich1991]). The second one is based on the fact that rays may intersect or the family of rays may have an envelope, but bicharacteristics may not. It allows to construct a formal asymptotic solutions that are valid in the neighbourhood of caustics and at caustics. This is the *method of Maslov's canonical operator* (see [Vainberg1989]).

We will present in the next section an example of the caustic formation for the scattering on a homogeneous disk and compare the geometrical optic solution with the wave field to confirm the fact that the wave field becomes strong on the caustic.

To find the location of a caustic one should solve the equation $J(\mathbf{x}) = 0$. It follows from the definition of the geometrical divergence (3.13) that the Hamiltonian system (3.9) is not sufficient to define the Jacobian J. Differentiating this system with respect to the initial parameter s we obtain

$$\begin{aligned}\frac{d}{ds}\left(\frac{d\mathbf{x}}{dt}\right) &= \nabla_p\nabla_x H(\mathbf{x},\mathbf{p})\frac{d\mathbf{x}}{dt} + \nabla_p\nabla_p H(\mathbf{x},\mathbf{p})\frac{d\mathbf{p}}{dt},\\ \frac{d}{ds}\left(\frac{d\mathbf{p}}{dt}\right) &= -\nabla_x\nabla_x H(\mathbf{x},\mathbf{p})\frac{d\mathbf{x}}{dt} - \nabla_x\nabla_p H(\mathbf{x},\mathbf{p})\frac{d\mathbf{p}}{dt}\end{aligned} \tag{3.17}$$

and will consider the Hamiltonian system (3.9) together with (3.17) which is

$$\frac{dx_1}{ds} = p_1, \quad \frac{dx_2}{ds} = p_2,$$

$$\frac{dp_1}{ds} = \frac{1}{2}\frac{\partial n}{\partial x_1}, \quad \frac{dp_2}{ds} = \frac{1}{2}\frac{\partial n}{\partial x_2},$$

$$\frac{d}{ds}\frac{dx_1}{dt} = \frac{dp_1}{dt}, \quad \frac{d}{ds}\frac{dx_2}{dt} = \frac{dp_2}{dt},$$

$$\frac{d}{ds}\frac{dp_1}{dt} = \frac{1}{2}\left(\frac{\partial^2 n}{\partial x_1^2}\frac{dx_1}{dt} + \frac{\partial^2 n}{\partial x_1\partial x_2}\frac{dx_2}{dt}\right),$$

$$\frac{d}{ds}\frac{dp_2}{dt} = \frac{1}{2}\left(\frac{\partial^2 n}{\partial x_1\partial x_2}\frac{dx_1}{dt} + \frac{\partial^2 n}{\partial x_2^2}\frac{dx_2}{dt}\right)$$

and corresponding initial conditions for $s = 0$

$$x_1(0) = x_1^0(t), \quad x_2(0) = x_2^0(t),$$

$$p_1(0) = p_1^0(t), \quad p_1(0) = p_1^0(t),$$

$$\frac{dx_1}{dt} = 0, \quad \frac{dx_2}{dt} = 0,$$

$$\frac{dp_1}{dt}(0) = \frac{dp_1^0(t)}{dt}, \quad \frac{dp_2}{dt}(0) = \frac{dp_2^0(t)}{dt}.$$

The solution of this system provides the family of rays $(x_1(t,s), x_2(t,s))$ together with values of the derivatives $(dx_1/dt(t,s), dx_2/dt(t,s))$.

Lemma 3.6.1 *The rays divergence is defined by the equation*

$$J(t,s) = p_1(t,s)\frac{dx_2}{dt}(t,s) - p_2(t,s)\frac{dx_1}{dt}(t,s). \tag{3.18}$$

Proof See [Tichonov1985, Engquist2003].

3.7 An example of a caustic

In the examples of the ray tracing we have already seen that rays may intersect, focus or the ray family may have an envelope. Now we calculate the caustic for the scattering of the parallel rays bundle on a homogeneous disk. The solution of the system (3.17) for the incident plane wave is shown on the Figure 3.10. The Figures 3.11,3.12 show the absolute value of the total field, which can be analytically found (see equations (2.4, 2.5)), calculated for two different wave numbers. As we mentioned above the wave field concentrates in some neighborhood of a caustic, what can be seen on the figures below. We mention that the value $n_{Snell} = 0.65$, which is the ratio of the refractive index value outside the disk to the value inside, corresponds to the refractive index $n = 2.37$.

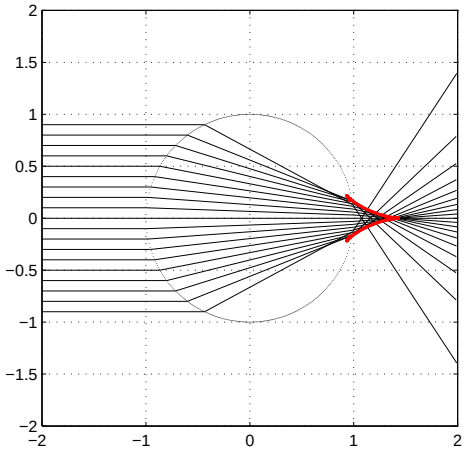

Figure 3.10: the rays tracing and the caustic (red curve) for $n_{Snell} = 0.65$.

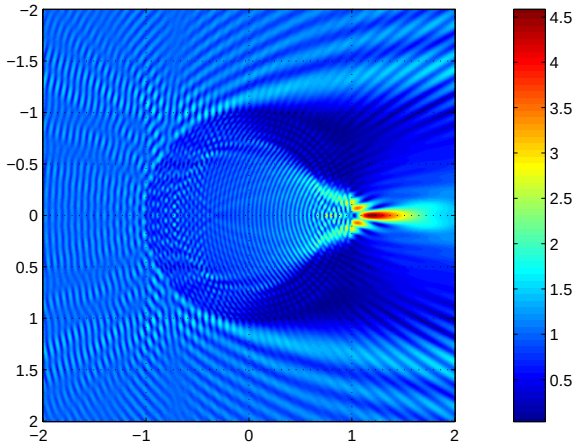

Figure 3.11: the absolute value of the total wave field $|u|$ for $k = 50, n = 1 + q, q = 1.37$.

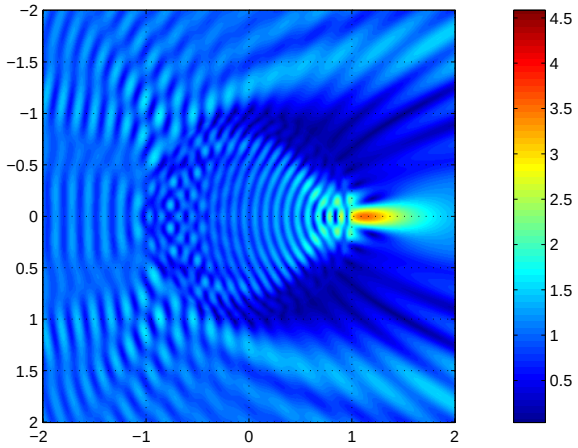

Figure 3.12: the absolute value of the total wave field $|u|$ for $k = 20, n = 1 + q, q = 1.37$.

Chapter 4

Error estimates

An important problem is to estimate in some suitable norm the difference between the eikonal approximation and the exact solution of the Helmholtz equation (2.1) with radiation condition (2.2) in terms of $1/k$.

This problem leads to the problem of finding an estimate for the solution of the inhomogeneous Helmholtz equation in terms of $1/k$. The estimates of this type can be found in the literature [Vainberg1989, Burq2002]. The Vainberg's and Burq's estimates for the resolvent of the Helmholtz equation are based on some special condition called the *non trapping condition* expressing a condition of the energy decay at infinity. Burq presented a new proof of the estimates given by Vainberg. For this reason we are not presenting both results and formulate the estimate following [Burq2002].

4.1 The Burq's 1/k estimate

Definition 4.1.1 *The energy $e \in \mathbb{R}^+$ is called non trapping if every bicharacteristic drawn on the surface $S_e = \{(\mathbf{x}, \mathbf{p}) : H(\mathbf{x}, \mathbf{p}) = e\}$ does leave any compact set in finite time ("leaving any compact set" means "going to the infinity in the $\mathbf{x}$ variable").*

There are other (equivalent to the presented here and to each other under some natural conditions) formulations of the non trapping condition. The detailed study of the non trapping conditions can be found in [Pauen2000].

Remark 4.1.1 *Let us note that the resolvent $R(z,k) = ((\Delta + k^2 n(\mathbf{x})) - z)^{-1}$ is defined and holomorphic for $Im z \neq 0$. Moreover it admits a meromorphic continuation as a bounded operator from $L_2(\mathbb{R}^2)$ to $L_{2,\mathrm{loc}}(\mathbb{R}^2)$ across the continuous spectrum $\mathbb{R}^+$ to the Riemann surface of the function $\ln z$ (which we will denote by $\widetilde{C}$).*

Proof See [Vainberg1989].

Definition 4.1.2 *The poles of the resolvent meromorphic continuation (4.1.1) are called resonances of the Helmholtz operator.*

Theorem 4.1.2 (Burq's estimate) *Consider a compact set $K \subset \mathbb{R}^+$. Suppose that every energy level $e \in K$ is non trapping. Then for any $N \in \mathbb{N}$ there exists $\varepsilon_N > 0$ such that for any $0 < 1/k < \varepsilon_N$ the Helmholtz operator $(\Delta + k^2 n(\mathbf{x}))$ has no resonance in the set*

$$\Lambda_N(k) = \{z \in \widetilde{C} : Rez \in K, |Imz| \leq N/k\}.$$

Moreover for any $\chi \in C_0^\infty(\mathbb{R}^2)$ and any $N \in \mathbb{N}$ there exists ε_N and $C > 0$ such that for any $0 < 1/k < \varepsilon_N$ and any $z \in \Lambda_N$

$$||\chi R(z,k)\chi||_{\mathcal{L}(L_2(\mathbb{R}^2))} \leq \frac{C}{k}. \tag{4.1}$$

Proof See [Burq2002].

Our goal is to estimate the error of the eikonal approximation: the difference between it and the exact solution of the problem (2.1,2.2) in terms of $1/k$. Unfortunately the Vainberg-Burq's estimate can not be used in our case. Vainberg shows in ([Vainberg1975]) that the non trapping condition implies the radiation condition (2.2) in some way, which is not satisfied by the error.

In the next section we present a new proof, which allows us to estimate the error in terms of $1/k$.

4.2 1/k estimate: initial-value approach

Considering the difference between the solution of the Helmholtz equation with the radiating conditions and the eikonal approximation we deduce that it is the subject of the initial value problem for the Helmholtz equation. It is known that although the Cauchy problem for the Helmholtz equation is uniquely solvable, it is notoriously unstable. Nevertheless the stabilized versions of the Cauchy problem play role in the numerical treatment of inverse problems (see, e.g., [Natterer1997, Natterer1995]).

So we are going to study an initial value problem for the Helmholtz equation

$$\begin{aligned} &(\Delta + k^2 n(\mathbf{x}))u = g(\mathbf{x}), \\ &u(x_1, 0) = 0, \quad \frac{\partial u}{\partial x_2}(x_1, 0) = 0 \end{aligned} \tag{4.2}$$

with g such that $supp(g) \subset B = [-r, r] \times [0, \infty)$ and $n(\mathbf{x}) = (1 + f(\mathbf{x}))$ such that $n(\mathbf{x}) \in C^\infty(\mathbb{R}^2)$, $n(\mathbf{x}) > 0$, $n(\mathbf{x}) = 1$ for $|\mathbf{x}| > R$ for some $R > 0$.

First we define u_k the low pass filtered version of u.

Definition 4.2.1 *Let $\widehat{u}(\xi_1, x_2)$ be the Fourier transform of u with respect to x_1:*

$$\widehat{u}(\xi_1, x_2) = \frac{1}{\sqrt{2\pi}} \int_{\mathbb{R}} \exp(-ix_1\xi_1) u(x_1, x_2) dx_1.$$

The u_k is called the low pass filtered version of u with the cut off frequency k if

$$\widehat{u}_k(\xi_1, x_2) = \begin{cases} \widehat{u}(\xi_1, x_2), |\xi_1| \leq k, \\ 0, \ \textit{otherwise.} \end{cases}$$

We will show that u_k is stably determined by g and admits estimate with constants, which tend to zero as $k \to \infty$

4.2.1 Homogeneous medium

We begin with the case of a constant refractive index, i.e. the problem

$$\begin{aligned} &(\Delta + k^2)u = g(\mathbf{x}), \\ &u(x_1, 0) = 0, \quad \frac{\partial u}{\partial x_2}(x_1, 0) = 0. \end{aligned} \tag{4.3}$$

For our application a constant refractive index is irrelevant. But dealing with this case yields some insight into the general case.

Theorem 4.2.1 *Let $u \in C^2(\mathbb{R}^2)$ be a solution of the Cauchy problem (4.3), then for p,q such that $1/p + 1/q = 1$ and $p > 4$ the following estimate is valid:*

$$||u_k||_{L_\infty(B)} \leq M_p k^{-2/p} ||g||_{L_q(B)}$$

with $M_p < \infty$.

Proof Applying the Fourier transform with respect to x_1 to the Cauchy problem (4.3) we obtain:

$$\begin{aligned} &\frac{\partial^2 \widehat{u}}{\partial x_2^2}(\xi_1, x_2) + (k^2 - \xi_1^2)\widehat{u}(\xi_1, x_2) = \widehat{g}(\xi_1, x_2), \\ &\widehat{u}(\xi_1, 0) = 0, \quad \frac{\partial \widehat{u}}{\partial x_2}(\xi_1, 0) = 0. \end{aligned} \tag{4.4}$$

This problem has the solution

$$\widehat{u}(\xi_1, x_2) = \frac{1}{\kappa} \int_{-\infty}^{x_2} \sin(\kappa(x_2 - x_2'))\widehat{g}(\xi_1, x_2')dx_2' \tag{4.5}$$

with $\kappa = \sqrt{k^2 - \xi_1^2}$. Note that κ is real for $|\xi_1| \leq k$, which is exactly where $\widehat{u} = \widehat{u}_k$.

Applying the inverse Fourier transform to the function (4.5) we arrive at the equation for the corresponding function $u_k(x_1, x_2)$:

$$\begin{aligned} u_k(x_1, x_2) &= \frac{1}{\sqrt{2\pi}} \int_{-\infty}^{x_2} \int_{-k}^{k} \frac{\sin(\kappa(x_2 - x_2'))}{\kappa} \widehat{g}(\xi_1, x_2') \exp(i\xi_1 x_1) d\xi_1 dx_2' \\ &= \int_{-\infty}^{x_2} \left(\widehat{K}_k(\cdot, x_2 - x_2')\widehat{g}(\cdot, x_2') \right)\widetilde{(}x_1) dx_2' \\ &= \frac{1}{\sqrt{2\pi}} \int_{-\infty}^{x_2} \left(K_k(\cdot, x_2 - x_2') * g(\cdot, x_2') \right)(x_1) dx_2', \end{aligned}$$

where we denoted by $\widehat{K}_k(\xi_1, x_2)$

$$\widehat{K}_k(\xi_1, x_2) = \begin{cases} \dfrac{\sin(\kappa x_2)}{\kappa}, |\xi_1| \leq k, \\ \\ 0, \text{ otherwise.} \end{cases}$$

Correspondingly we have

$$K_k(x_1, x_2) = \frac{1}{2\pi} \int_{-k}^{k} \frac{\sin(\kappa x_2)}{\kappa} \exp(i\xi_1 x_1) d\xi_1.$$

Thus,

$$u_k(x_1, x_2) = \int_{-\infty}^{x_2} \int_{-\infty}^{+\infty} K_k(x_1 - x_1', x_2 - x_2') g(x_1', x_2') dx_1' dx_2'.$$

Now consider p, q such that $1/p + 1/q = 1$. For $x_2 \leq r$ we have:

$$|u_k(\mathbf{x})| \leq$$
$$\left(\int_{-\infty}^{x_2} \int_{-\infty}^{+\infty} |K_k(x_1 - x_1', x_2 - x_2')|^p dx_1' dx_2' \right)^{1/p} \left(\int_{-\infty}^{x_2} |g(x_1', x_2')|^q dx_1' dx_2' \right)^{1/q}$$

$$\leq ||K_k||_{L^p(\mathbb{R}^2)} ||g||_{L_q([-r,r]\times[0,r])}.$$

To estimate $|K_k(\mathbf{x})|$ we rewrite $K_k(\mathbf{x})$ in the form

$$K_k(x_1, x_2) = \frac{1}{4i\pi} \left(\int_{-k}^{k} \left(\frac{\exp(i\xi_1 x_1 + i\kappa x_2)}{\kappa} - \frac{\exp(i\xi_1 x_1 - i\kappa x_2)}{\kappa} \right) d\xi_1 \right) =$$

$$\frac{1}{4i\pi} \left(\int_{-k}^{k} \left(\frac{\exp(i|\mathbf{x}|(\xi_1 x_1/|\mathbf{x}| + \kappa x_2/|\mathbf{x}|))}{\kappa} - \frac{\exp(i|\mathbf{x}|(\xi_1 x_1/|\mathbf{x}| - \kappa x_2/|\mathbf{x}|))}{\kappa} \right) d\xi_1 \right) =$$

$$K_k^1(x_1, x_2) - K_k^2(x_1, x_2).$$

The integrals $K_k^1(x_1, x_2)$ and $K_k^2(x_1, x_2)$ are estimated independently by the stationary phase method ([Borovikov1994]). We conclude that there is a constant $M < \infty$ such that for $|\mathbf{x}| \to \infty$

$$|K_k(\mathbf{x})| \leq M(1 + k|\mathbf{x}|)^{-1/2}.$$

Hence, for $p > 4$

$$\begin{aligned} ||K_k||_{L^p(\mathbb{R}^2)} &\leq M \left(\int_{\mathbb{R}^2} (1 + k|\mathbf{x}|)^{-p/2}) d\mathbf{x} \right)^{1/p} \\ &= M k^{-2/p} \left(\int_{\mathbb{R}^2} (1 + |\mathbf{y}|)^{-p/2}) d\mathbf{y} \right)^{1/p} \\ &= M_p k^{-2/p} \end{aligned}$$

with some constant $M_p < \infty$. Due to this inequality yields

$$||u_k||_{L_\infty(B)} \leq M_p k^{-2/p} ||g||_{L_q(B)}. \tag{4.6}$$

□

We note that the estimate (4.6) is valid for $p > 4$, thus we estimated the low pass filtered solution by an expansion close to $Ck^{-1/2}||g||_{L_q(B)}$ with some constant C. To estimate u_k by terms of order $1/k$ we need some other considerations.

Theorem 4.2.2 *Let $u \in C^2(\mathbb{R}^2)$ be a solution of the Cauchy problem (4.3) and $0 \leq x_2 \leq r$, then*

$$||u_{\zeta k}(\cdot, x_2)||^2_{L_2(-r,r)} \leq \frac{r}{k^2(1-\zeta^2)} ||g||^2_{L_2([-r,r]\times[0,r])}$$

for each $0 < \zeta < 1$.

Proof The Fourier transform of the solution u can be written in the form (4.5):

$$\widehat{u}(\xi_1, x_2) = \frac{1}{\kappa} \int_{-\infty}^{x_2} \sin(\kappa(x_2 - x_2')) \widehat{g}(\xi_1, x_2') dx_2'$$

with $\kappa = \sqrt{k^2 - \xi_1^2}$. Thus, for $|\xi_1| \leq \zeta k$ with $0 < \zeta < 1$ and $|x_2| \leq r$

$$|\widehat{u}(\xi_1, x_2)|^2 \leq \frac{r}{k^2(1-\zeta^2)} \int_0^r |\widehat{g}(\xi_1, x_2)|^2 dx_2'.$$

Therefore,

$$||u_{\zeta k}(\cdot,x_2)||^2_{L_2(-r,r)} = \int\limits_{-\zeta k}^{\zeta k} |\widehat{u}(\xi_1,x_2)|^2 d\xi_1$$
$$\leq \frac{r}{k^2(1-\zeta^2)} \int\limits_{-\zeta k}^{\zeta k}\int\limits_{0}^{r} |\widehat{g}(\xi_1,x_2')|^2 dx_2' d\xi_1$$
$$\leq \frac{r}{k^2(1-\zeta^2)} ||g||^2_{L_2([-r,r]\times[0,r])}.$$

□

4.2.2 Nonhomogeneous medium

Now turn to the case (4.2) with a nonconstant refractive index.

Theorem 4.2.3 *Let $f(\mathbf{x})$ be a function such that $f \in C^1$, f vanishes outside B, $-1 < m < f < +\infty$, $|\partial f/\partial x_2| < M < +\infty$.*

Then for the low pass filtered version of the solution of the Cauchy problem (4.2) the following estimate holds

$$||u_{\zeta' k}(\cdot,x_2)||^2_{L_2(-r,r)} \leq \frac{C(r)}{k^2\zeta'^2} ||g||^2_{L_2(B)}$$

for every constant $0 < \zeta' < \sqrt{1+m}$.

Proof First we estimate the solution for the case of a piecewise constant as a function of x_2 function f, namely

$$f(x_1,x_2) = f_i(x_1), \quad ih \leq x_2 \leq (i+1)h \tag{4.7}$$

with some $h > 0$.

Applying the Fourier transform with respect to x_1 to the Cauchy problem (4.2) we arrive for $ih \leq x_2 \leq (i+1)h$ to

$$\frac{d^2\widehat{u}}{dx_2^2}(\cdot,x_2) + A_i\widehat{u}(\cdot,x_2) = \widehat{g}(\cdot,x_2), \tag{4.8}$$

$$\widehat{u}(\xi_1,0) = 0, \quad \frac{\partial\widehat{u}}{\partial x_2}(\xi_1,0) = 0,$$

with the operator A_i in $L_2(\mathbb{R}^2)$ defined by

$$(A_i v)(\xi_1) = (k^2 - \xi_1^2)v(\xi_1) + (2\pi)^{-1/2}k^2(\widehat{f}_i * v)(\xi_1). \tag{4.9}$$

The operator A_i is selfadjoint since $f(\mathbf{x})$ is realvalued. Moreover, by the Parseval's relation

$$(\widehat{f_i} * v, v)_{L_2(\mathbb{R}^1)} = \int_{-\infty}^{\infty} (\widehat{f_i} * v)\overline{v} d\xi_1 = \int_{-\infty}^{\infty} (\widehat{f_i} * v)\overline{\widetilde{v}} dx_1$$

$$= (2\pi)^{1/2} \int_{-\infty}^{\infty} f_i |\widetilde{v}|^2 dx_1 \geq (2\pi)^{1/2} m(v, v)_{L_2(\mathbb{R}^1)}$$

with $\widetilde{v}$ the inverse Fourier transform. Thus, for the restriction of the operator A_i to $L_2(-\kappa, \kappa)$, which will be still denoted by A_i, we have the estimate

$$(A_i v, v)_{L_2(-\kappa,\kappa)} \geq (k^2 - \kappa^2 + k^2 m)(v, v)_{L_2(-\kappa,\kappa)} \tag{4.10}$$

with $\kappa = \sqrt{k^2 - \xi_1^2}$.

Integrating (4.8) over $[ih, x_2]$ we obtain

$$\widehat{u}(\cdot, x_2) = \cos\left(K_i(x_2 - ih)\right) \widehat{u}(\cdot, x_2) + K_i^{-1} \sin\left(K_i(x_2 - ih)\right) \frac{\partial \widehat{u}}{\partial \xi_1}(\cdot, x_2)$$

$$+ \int_{ih}^{x_2} K_i^{-1} \sin\left(K_i(x_2 - x_2')\right) \widehat{g}(\cdot, x_2') dx_2'$$

with $K_i = \sqrt{A_i}$. This equation makes sense for the positive definite A_i which is the case for $(k^2 - \kappa^2 + k^2 m) > 0$. For $|\xi_1| < k$ we put

$$U_i(\xi_i) = \begin{pmatrix} \widehat{u}(\xi_1, ih) \\ \dfrac{\partial \widehat{u}}{\partial x_2(\xi_1, ih)} \end{pmatrix}$$

and from the last equation for the $\widehat{u}(\cdot, x_2)$ we obtain

$$U_{i+1} = L_i U_i + \int_{ih}^{(i+1)h} J_i(x_2') \widehat{g}(\cdot, x_2') dx_2', \tag{4.11}$$

where

$$L_i = \begin{pmatrix} \cos(K_i h) & K_i^{-1} \sin(K_i h) \\ -K_i \sin(K_i h) & \cos(K_i h) \end{pmatrix},$$

and

$$J_i(x_2') = \begin{pmatrix} K_i^{-1} \sin\left(K_i((i+1)h - x_2')\right) \\ \cos\left(K_i((i+1)h - x_2')\right) \end{pmatrix}.$$

Solving the recursion (4.11) yields

$$U_i = L_{i-1} \dots L_0 U_0 + \sum_{j=0}^{i-1} L_i \dots L_{j+1} \int_{jh}^{(j+1)h} J_j(x_2')\widehat{g}(\xi_1, x_2)dx_2'.$$

We note that $L_i = D_i Q_i D_i^{-1}$ with

$$Q_i = \begin{pmatrix} \cos(K_i h) & \sin(K_i h) \\ -\sin(K_i h) & \cos(K_i h) \end{pmatrix}$$

and

$$D_i = \begin{pmatrix} I & 0 \\ 0 & K_i \end{pmatrix}.$$

Since $U_0 = 0$ we need to consider only $L_i \dots L_{j+1} J_j(x_2')$.

$$\begin{aligned} & L_i \dots L_{j+1} J_j(x_2') \\ & = D_i Q_i D_i^{-1} D_{i-1} \dots D_{j+2}^{-1} D_{j+1} Q_{j+1} \begin{pmatrix} K_j^{-1} \sin\left(K_j((j+1)h - x_2')\right) \\ K_{j+1}^{-1} \cos\left(K_j((j+1)h - x_2')\right) \end{pmatrix} \\ & = D_i M_{ij}, \end{aligned}$$

where by M_{ij} we denote

$$M_{ij} = Q_i D_i^{-1} D_{i-1} \dots D_{j+2}^{-1} D_{j+1} Q_{j+1} \begin{pmatrix} K_j^{-1} \sin\left(K_j((j+1)h - x_2')\right) \\ K_{j+1}^{-1} \cos\left(K_j((j+1)h - x_2')\right) \end{pmatrix}.$$

To estimate the euclidean norm $||\cdot||$ of M_{ij} first we mention that

$$||Q_i|| = 1. \tag{4.12}$$

Next we estimate the norm $||D_i^{-1} D_{i-1}||$. Since $|\partial f/\partial x_2| < \infty$ and $|f| < \infty$,

$$||f_i - f_{i+1}||_{L_2(\mathbb{R}^2)} \le h c_f,$$

with some constant $0 < c_f < \infty$. Hence the similar estimate holds for $||A_i||$ and, consequently,

$$||K_i K_{i+1}|| \le 1 + h c_1.$$

Thus, the following estimate holds

$$||D_i^{-1} D_{i-1}|| \le 1 + ch \tag{4.13}$$

with some constant c.

To estimate terms containing K_i^{-1} we remind that

$$(k^2 - \kappa^2 + k^2 m) > 0$$

has to be fulfilled. That is $k\sqrt{1+m} > \kappa$ or

$$\kappa = k\zeta_1\sqrt{1+m}$$

with some $0 < \zeta_1 < 1$. On the other hand, the operators A_i are selfadjoint, that is for every i A_i has a complete system of eigenfunctions. For a eigenfunction v_i of A_i by use of (4.10) holds

$$||v_i||^2 \geq k^2 - \kappa^2 + k^2 m = k^2(1+m)(1-\zeta_1^2), \tag{4.14}$$

which gives estimates for the terms containing K_i^{-1}.

Now putting together the estimates (4.12), (4.13) and (4.14) we get the estimate for $||M_{ij}||$:

$$||M_{ij}|| \leq \frac{(1+ch)^{i-j+1}}{k\zeta'}$$

with $\zeta' = \sqrt{1+m}\sqrt{1-\zeta_1^2}$.

Thus, we get

$$U_i = D_i \sum_{j=0}^{i-1} \int_{jh}^{(j+1)h} M_{ij}(x_2')\widehat{g}(jx_2')dx_2',$$

which implies for $\widehat{u}(\xi, ih)$

$$\begin{aligned}
|\widehat{u}(\xi, ih)| &\leq \frac{1}{k\zeta'} \sum_{j=0}^{i-1} (1+ch)^{i-j+1} \int_{jh}^{(j+1)h} |\widehat{g}(\xi_1, x_2')|dx_2' \\
&\leq \frac{1}{k\zeta'}(1+ch)^{i+1} \int_0^{ih} |\widehat{g}(\xi_1, x_2')|dx_2' \\
&\leq \frac{1}{k\zeta'} \exp((i+1)ch)\sqrt{ih} \left(\int_0^{ih} |\widehat{g}(\xi_1, x_2')|^2 dx_2' \right)^{1/2}.
\end{aligned}$$

For $ih = x_2 \leq r$ it follows that

$$|\widehat{u}(\xi_1, x_2)|^2 \leq \frac{r\exp(2(r+1)c)}{k^2\zeta'^2} \int_0^r |\widehat{g}(\xi_1, x_2')|dx_2'$$

and finally for $u_{k\zeta'}(\cdot, x_2)$

$$||u_{\zeta' k}(\cdot, x_2)||^2_{L_2(-r,r)} \leq \frac{r \exp(2(r+1)c)}{k^2 \zeta'^2} ||g||^2_{L_2(B)}. \tag{4.15}$$

To treat the general case we mention that the constant c in the estimate (4.15) does not depend on h (see estimates (4.12, 4.13, 4.14)). Thus, letting $h \to 0$ we derive the estimate (4.15) for the case with an arbitrary (not necessarily piecewise constant) function $f(\mathbf{x})$. $\square$

4.3 Error estimate for the eikonal approximation

Now we can estimate the error of the eikonal approximation for the case of the refractive index $n(\mathbf{x}) = 1 + f(\mathbf{x})$ with $n(\mathbf{x}) \in C^\infty(\mathbb{R}^2)$, $n(\mathbf{x}) > 0$, $n(\mathbf{x}) = 1$ for $|\mathbf{x}| > R$ for some $R > 0$. We deal with the plane incident wave $u_i(\mathbf{x}) = \exp(ikx_1)$. In [Vainberg1975] the following theorem is proven.

Theorem 4.3.1 *Let supp$(1 - n(\mathbf{x})) \subset \Omega$, where Ω be a domain outside a neighbourhood of the caustic. Assume also that the non trapping condition (4.1.1) is satisfied. Then for the solution $u(\mathbf{x})$ of the Helmholtz equation (2.1) with the radiating condition (2.2) yields*

$$u(\mathbf{x}) = \frac{1}{\sqrt{J(\mathbf{x})}} \exp(ik\phi(\mathbf{x})) + v(\mathbf{x}), \tag{4.16}$$

where v tends to zero uniformly in $x \in \Omega$ as $k \to \infty$. Here $J(\mathbf{x})$ is the geometrical divergence and $\phi(\mathbf{x})$ is the eikonal.

Remark 4.3.2 *By writing $\phi(\mathbf{x})$ we mean following: Take a wave front $x_2 = -\widetilde{R}$ with $\widetilde{R} > R$ and fix it. Consider the ray $\gamma_x(s)$ starting on the wave front and ending at the point $\mathbf{x}$: $\gamma_x(s_x) = \mathbf{x}$ and calculate the value of the eikonal over this ray starting on the given wave front by the formula (3.11):*

$$\phi(\mathbf{x}) = \int_0^{s_x} \sqrt{n(\gamma_x(s))} ds.$$

The proof of this theorem is rather complicated and the result does not give an estimate of the error function $v(\mathbf{x})$ in terms of $1/k$. With the help of the $1/k$-estimate (4.15) we can estimate of the function $v(\mathbf{x})$ in terms of the small parameter $1/k$ in a domain containing no caustics. Moreover we do not need the non trapping condition here.

Theorem 4.3.3 *In every band $B = [-R, R] \times [0, \infty)$, $R > 0$ containing no caustic, the function $v(\mathbf{x})$ allows the following estimation:*

$$||v_{\zeta' k}(\mathbf{x})||^2_{L_2(-R,R)} \leq \frac{C}{k^2 \zeta'^2} ||\Delta A(\mathbf{x})||^2_{L_2(B)}, \tag{4.17}$$

with the amplitude of the eikonal approximation $A(\mathbf{x}) = \left(\sqrt{J(\mathbf{x})}\right)^{-1}$, and positive constants ζ' and C.

Proof Putting the function $v(\mathbf{x})$ in the Helmholtz equation and using the eikonal equation (3.2)

$$|\nabla\phi(\mathbf{x})|^2 - n(\mathbf{x}) = 0$$

and the transport equation (3.3)

$$2\nabla\phi\nabla A + A\Delta\phi = 0$$

we see that $v(\mathbf{x})$ solves the equation

$$\Delta v(\mathbf{x}) + k^2 n(\mathbf{x}) v(\mathbf{x}) = -\Delta A(\mathbf{x}) \exp(ik\mathbf{x}).$$

Moreover for the refractive index $n(\mathbf{x})$ under consideration it solves the initial value problem for this equation with zero initial values. Thus, we can apply the $1/k$-estimate (4.15) for the solution of the initial value problem we get the desired estimate. □

Chapter 5

Perturbed refractive index

In many applications the real model can be understood as a "small" perturbation of some other model with known parameters (rays, eikonal etc.) The natural treatment of such models is by using the *perturbation methods*. We concern the eikonal perturbation due to the refractive index perturbation.

Perturbation methods are widely used in seismology (see, for example, [Snieder1992, Farra1989a, Farra1989b, Cerveny1982]), where the computation of rays, eikonal and other physical attributes for the real structures is complicated and time consuming.

5.1 Hamiltonian treatment

Following [Farra1987, Farra1999] we present an often used treatment.

We assume that the reference model is characterized by the refractive index $n_0(\mathbf{x})$ and consider perturbation of the model such that the refractive index is changed to $n(\mathbf{x})$. Then the Hamiltonian is changed from

$$H_0 = \frac{1}{2}(\mathbf{p}^2 - n_0)$$

to

$$H = \frac{1}{2}(\mathbf{p}^2 - n) = H_0 - \frac{n - n_0}{2}.$$

Following the perturbation theory procedure we identify a small parameter ε, such that for $\varepsilon = 0$ we deal with the reference problem. Thus, we assume that the perturbed refractive index is $n(\mathbf{x}) = n_0(\mathbf{x}) + \varepsilon n_1(\mathbf{x})$.

One of the standard results is as follows: For the perturbed eikonal to the first order in ε yields:

$$\phi(\mathbf{x}_1, \mathbf{x}_0) \sim \int_{x_0}^{x_1} n_0(\gamma_0(s))ds + \frac{\varepsilon}{2}\int_{x_0}^{x_1} n_1(\gamma_0(s))ds, \tag{5.1}$$

where the integrals are taken along the non perturbed ray γ_0.

We give a heuristic derivation of (5.1) along the lines of [Farra1999].

We write the perturbed Hamiltonian H in the perturbation series in powers of ε:

$$H = H_0 + \varepsilon H_1 + \varepsilon^2 H_2 + \dots,$$

where obviously $H_1 = -n_1(\mathbf{x})/2$ and $H_j = 0$ for all $j \geq 2$.

Denoting by $(\mathbf{x}_0(s), \mathbf{p}_0(s))$ the solution of the Hamiltonian system (3.9) with the Hamiltonian function H_0 and corresponding initial conditions we present the perturbed solution $(\mathbf{x}(s), \mathbf{p}(s))$ of the Hamiltonian system with the same initial conditions and the perturbed Hamiltonian H in a form

$$(\mathbf{x}(s), \mathbf{p}(s)) = (\mathbf{x}_0(s) + \delta\mathbf{x}(s), \mathbf{p}_0(s) + \delta\mathbf{p}(s)),$$

where the perturbation $(\delta\mathbf{x}(s), \delta\mathbf{p}(s))$ can be expanded in a perturbation series in powers of ε

$$\begin{aligned} \delta\mathbf{x}(s) &= \varepsilon x_1(s) + \varepsilon^2 x_2(s) + \dots, \\ \delta\mathbf{p}(s) &= \varepsilon p_1(s) + \varepsilon^2 p_2(s) + \dots. \end{aligned} \tag{5.2}$$

We remaind that in terms of the solution of the Hamiltonian equation $(\mathbf{x}, \mathbf{p})$ the eikonal is obtained by

$$\phi(\mathbf{x}_1, \mathbf{x}_0) = \int_{x_0}^{x_1} \mathbf{p} \cdot \dot{\mathbf{x}} ds, \tag{5.3}$$

where the integration is taken over the ray connecting points $\mathbf{x}_0$ and $\mathbf{x}_1$. Using the perturbation series (5.2) we can write to the first order in ε

$$\mathbf{p} \cdot \dot{\mathbf{x}} = \mathbf{p}_0 \cdot \dot{\mathbf{x}}_0 + \varepsilon(\mathbf{p}_0 \cdot \dot{\mathbf{x}}_1 + \mathbf{p}_1 \cdot \dot{\mathbf{x}}_0). \tag{5.4}$$

Now putting together (5.3) and (5.4) we get the expression for the eikonal to the first order in ε

$$\phi(\mathbf{x}_1, \mathbf{x}_0) = \phi_0(\mathbf{x}_1, \mathbf{x}_0) - \int_{x_0}^{x_1} \varepsilon H_1 ds,$$

where H_1 is computed at $(\mathbf{x}_0, \mathbf{p}_0)$, i.e., over the non perturbed ray. That is, to the first order the perturbed eikonal has the approximation [Farra1999]:

$$\phi(\mathbf{x}_1, \mathbf{x}_0) = \int_{x_0}^{x_1} n_0(\gamma_0(s)) ds + \frac{\varepsilon}{2} \int_{x_0}^{x_1} n_1(\gamma_0(s)) ds,$$

where the integrals are taken along the non perturbed ray γ_0.

The formula (5.1) is well-known and widely used is numerical computations. However the derivation involves many unproved conclusions. To our knowledge it was never rigorously proved. We are going to give such a proof of it in the next section.

5.2 Perturbation of the eikonal function

Let us consider a perturbed medium characterized by the refractive index n and let n_0 be the refractive index of the reference medium, $n - n_0$ its small perturbation. The corresponding eikonal functions fulfill the equations

$$|\nabla \phi_0|^2 = n_0,$$

and

$$|\nabla \phi|^2 = n.$$

We assume that for the eikonal functions the same initial data is given on the wave front (same for both eikonals) Γ with a smooth curve $\Gamma \in C^1$ outside Ω. Since on the wave front the initial data is some constant we can assume without loss of generality that $\phi|_\Gamma = \phi_0|_\Gamma = 0$. Writing $\phi(\mathbf{x})$ we mean the value of the eikonal calculated by

$$\phi(\mathbf{x}) = \int_0^{s_x} \sqrt{n(\gamma_x(s))} ds,$$

where the ray γ_x of the perturbed medium starts on the wave front Γ and ends at the point $\mathbf{x}$: $\gamma_x(s_x) = \mathbf{x}$ (and analogously for $\phi_0(\mathbf{x})$).

Our goal is to give a formal proof of the formula (5.1). To do it we need the *implicit function theorem.*

Lemma 5.2.1 (The implicit function theorem) *Let $\Psi : U_1 \to U_2$ be a Fréchet differentiable map acting between two Banach spaces. Suppose that for some $f_0 \in U_1$ the Fréchet differential Ψ' is invertible. Then there are neighbourhoods $\widetilde{U}_1$ of f_0 and $\widetilde{U}_2$ of $g_0 = \Psi f_0$, such that Ψ is one-to-one mapping between $\widetilde{U}_1$ onto $\widetilde{U}_2$ and the inverse map Ψ^{-1} is Fréchet differentiable in $\widetilde{U}_2$. Moreover, the differential $\Psi'(f)$ is invertible for all $f \in \widetilde{U}_1$ and for the family of inverses holds:*

$$(\Psi'(f))^{-1} = (\Psi^{-1})'(g), \quad g = \Psi(f).$$

Proof See [Hamilton1982].

Now we are ready to proof the following theorem.

Theorem 5.2.2 *Consider $\Omega \subset\subset \mathbb{R}^2$ and let the functions $n_0(\mathbf{x}), n(\mathbf{x}) \in C^1(\overline{\Omega})$ satisfy*

$$\begin{array}{ll} (i) & n_0(\mathbf{x}) > \rho > 0 \quad \forall \mathbf{x} \in \Omega \\ (ii) & \varepsilon = ||n(\mathbf{x}) - n_0(\mathbf{x})||_{C^1(\overline{\Omega})} \text{ is small.} \end{array}$$

Then for the perturbed eikonal function we have:

$$\phi(\mathbf{x}) = \phi_0(\mathbf{x}) + \frac{1}{2}\int_{\gamma_0}(n - n_0)(\gamma_0(s))ds + O(\varepsilon^2), \tag{5.5}$$

where the integral is taken along the non perturbed ray γ_0 which comes to $\mathbf{x}$ and the functions $\phi_0, \phi \in C^2(\overline{\Omega})$ are defined above.

Proof Consider the space $\mathcal{H} = \{\phi \in C^2(\overline{\Omega}) : \phi|_\Gamma = 0\}$ and the operator $\Psi : \mathcal{H} \to C^1(\overline{\Omega})$

$$\Psi(\phi) = |\nabla\phi|^2.$$

Because of

$$|\nabla(\phi + h)|^2 = (\nabla\phi, \nabla\phi) + 2(\nabla\phi, \nabla h) + (\nabla h, \nabla h), \tag{5.6}$$

where $(\cdot, \cdot)$ is the euclidian scalar product, the operator Ψ is Fréchet differentiable and

$$\Psi'(\phi)h = 2(\nabla\phi, \nabla h).$$

To apply the implicit function theorem for Ψ at some ϕ_0 we have to show that $\Psi'(\phi_0)$ is invertible. We remark that for $|\nabla\phi_0| > \sqrt{\rho} > 0$

$$(\nabla\phi_0, \nabla h) = |\nabla\phi_0|\nabla_{\nabla\phi_0}h,$$

where $\nabla_{\nabla\phi_0}h$ is the directional derivative of h in the direction $\nabla\phi_0/|\nabla\phi_0|$. Thus, the inverse $(\Psi'(\phi_0))^{-1}$ is

$$(\Psi'(\phi_0))^{-1}(g) = \frac{1}{2}\int_{\gamma_0} g(\gamma_0(s))ds,$$

where the integral is taken along the characteristic γ_0 corresponding to $n_0 = |\nabla\phi_0|^2$ (see, e.g.,[Arnold1989]).

Hence, $\Psi'(\phi_0)$ is invertible and by the implicit function theorem, Ψ is invertible in a neigbourhood of

$$\Psi(\phi_0) = n_0$$

and the inverse $\Phi = \Psi^{-1}$ is Fréchet differentiable. The operator $\Phi : C^1(\overline{\Omega}) \to \mathcal{H}$ is the solution operator of

$$|\nabla\phi|^2 = n, \quad \phi|_\Gamma = 0, \tag{5.7}$$

i.e., $\phi = \Phi(n)$.

Remark 5.2.3 *The problem (5.7) is uniquely solvable up to the sign of the solution (see Section 3.4). Let us take a solution ϕ_0 corresponding to n_0 and fix it. By the implicit function theorem there are neighbourhoods of n_0 and ϕ_0 such that the operator Ψ is one-to-one mapping and our following results are true. The same considerations hold for the other solution of the problem (5.7) corresponding to n_0.*

Since the operator Φ is Fréchet differentiable, then for a small enough $\varepsilon = ||n - n_0||_{C^1(\overline{\Omega})}$ we have for the solution ϕ of $|\nabla\phi|^2 = n$, $\phi|_\Gamma = 0$

$$\Phi(n) = \Phi(n_0) + \Phi'(n_0)(n - n_0) + o(\varepsilon). \tag{5.8}$$

To get the better error estimate in the (5.8) we note that by (5.6) the operator Ψ is even twice Fréchet differentiable. It means that for the small enough $\varepsilon_1 = ||\phi - \phi_1||_{C^2(\overline{\Omega})}$ holds:

$$\Psi(\phi) = \Psi(\phi_1) + \Psi'(\phi_1)(\phi - \phi_1) + O(\varepsilon_1^2). \tag{5.9}$$

Now take

$$\phi_1 = \Phi'(n_0)(n - n_0).$$

Since the differential is a bounded linear operator, $\phi_1 = O(\varepsilon)$. Thus, for $\phi = \phi_0 + \phi_1$ the expression (5.9) is:

$$\Psi(\phi_0 + \phi_1) = \Psi(\phi_0) + \Psi'(\phi_0)\phi_1 + O(\varepsilon^2),$$

or in the other terms:

$$\Psi(\phi_0 + \phi_1) = n_0 + (n - n_0) - n_2,$$

where $n_2 = O(\varepsilon^2)$ and we used the relation $\Psi'(\phi_0) = (\Phi'(n_0))^{-1}$.

Thus,

$$n = \Psi(\phi_0 + \phi_1) + n_2.$$

For a small enough ε, $|\nabla(\phi_0 + \phi_1)| > \sqrt{\rho_1} > 0$. Therefore we conclude from the implicit function theorem that the operator Ψ is invertible in the neigbourhood of $\Psi(\phi_0 + \phi_1)$. Applying the inverse operator Φ to the last equation we get:

$$\Phi(n) = \Phi(\Psi(\phi_0 + \phi_1) + n_2) = (\phi_0 + \phi_1) + \Phi'(\Psi(\phi_0 + \phi_1))(n_2) + O(\varepsilon^2).$$

Again, since the Fréchet differential is a bounded linear operator, $\Phi'(\Psi(\phi))(n_2) = O(\varepsilon^2)$. Hence we have:

$$\Phi(n) = \phi_0 + \phi_1 + O(\varepsilon^2),$$

where

$$\phi_1 = \Phi'(n_0)(n - n_0) = \frac{1}{2}\int_{\gamma_0} (n - n_0)(\gamma_0(s))ds$$

and integral is taken along the characteristic γ_0 corresponding to n_0. □

Chapter 6

Ultrasound tomography

In ultrasound tomography the aim is to reconstruct an image, a cross section of the object, from the data obtained when the ultrasound passes through the object. The measured pulses will be changed due to the properties of the media such as refractive index.

In contrast to the direct scattering problem described in the section 2.2.1, where the refractive index is known and the task is to determine the scattered field, here we know scattered field and want to recover the refractive index. For this reason this problem is called *inverse scattering problem.*

6.1 The inverse scattering problem

As we already mentioned above in the inverse scattering problem the refractive index $n(\mathbf{x})$ with $supp(1-n) \subset \Omega = B(R)$ is unknown. We want to get information about it (see Figure 6.1) by probing the object with plane incident waves $u_i = \exp(ik\boldsymbol{\theta}\mathbf{x})$, $\boldsymbol{\theta} = (\cos\theta, \sin\theta)$ and measuring over Γ^+ the resulting wave field $g_\theta = u$ for different directions $\boldsymbol{\theta}$.

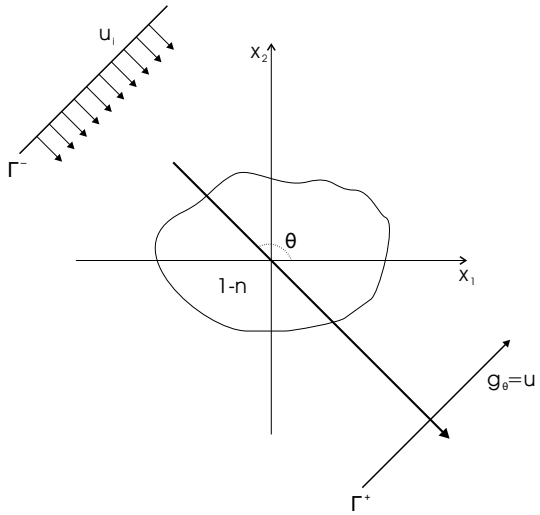

Figure 6.1: Basic geometry: $\boldsymbol{\theta} = (\cos\theta, \sin\theta)$ is the direction of the incident plane wave.

Here the measured scattered wave field satisfies the Helmholtz equation (2.1)

$$\Delta u + k^2 n u = 0$$

and $u = u_i + u_s$ with the scattered term u_s, which satisfies the radiation condition (2.2)

$$\lim_{r\to\infty} \sqrt{r}\left(\frac{\partial u_s}{\partial r} - iku_s\right) = 0.$$

Assume that the scattered wave field is known at a fixed k for all incident directions. Our task is to reconstruct n from these data.

Uniqueness for the inverse scattering problem was stated by Nachman [Nachman1988] in the following way.

For a bounded domain $\Omega \subset \mathbb{R}^2$ with the smooth boundary $\partial\Omega$ we consider the Dirichlet problem

$$\begin{aligned} &\Delta u + k^2 n u = 0 \text{ in } \Omega, \\ &u|_{\partial\Omega} = g. \end{aligned} \tag{6.1}$$

Remark 6.1.1 *In general the problem (6.1) is not uniquely solvable. For example consider $n(\mathbf{x}) = 1$ for all $\mathbf{x} \in \mathbb{R}^2$, $\Omega = B(1)$ and $g = 0$.Let k be a zero of a Bessel function J_q. Then the functions $u_1 = 0$ and $u_2(r,\varphi) = J_q(kr)\exp(iq\varphi)$ are the solutions of the problem (6.1). It means that for some cases the Dirichlet problem has eigenvalues. To avoid the nonuniqueness we assume that in our case the problem (6.1) is uniquely solvable.*

For a function $g \in H^{1/2}(\partial\Omega)$ let us consider the solution u of the Dirichlet problem (6.1). We define the *Dirichlet to Neumann map* Λ_n by

$$\Lambda_n(g) = \left.\frac{\partial u}{\partial \nu}\right|_{\partial\Omega},$$

where ν denotes the external normal to $\partial\Omega$.

The inverse scattering problem is to determine the refractive index n knowing Λ_n.

Theorem 6.1.2 (Nachman) *Let $n \in L^p_\rho(\mathbb{R}^2)$ $(1 < p < 2, \rho > 1)$ be a function of the form $n = (\Delta h)/h$ with $h \in L_\infty(\mathbb{R}^2)$ and $h(\mathbf{x}) > c_0 > 0$. Then $\Lambda_{n_1} = \Lambda_{n_2}$ yields $n_1 = n_2$.*

Proof The idea of the Nachman's proof [Nachman1988] is follows. He defines the family of exponentially growing solutions $u(\mathbf{x}, \omega)$ of the Helmholtz equation and introduces the *scattering transform*

$$T(w) = \int\limits_{\mathbb{R}^2} \exp(-iwz)u(\mathbf{x}, w)n(\mathbf{x}) \exp(i(wz + \overline{wz}))d\mathbf{x},$$

where $w \in \mathbb{C}\backslash\{0\}$ and for $\mathbf{x} = (x_1, x_2)$ $z = x_1 + ix_2$. He shows that for n of the form $n = (\Delta h)/h$ the scattering transform $T(w)$ exists. Then he applies the so-called $\overline{\partial}$-method, introduced by Beals and Coifman [Beals1986], to recover n from $T(w)$ known for all $w \in \mathbb{C} \setminus \{0\}$. The more detailed discussions on the $\overline{\partial}$-method can be found in [Novikov1987].

Remark 6.1.3 *In contrast to the Theorem 6.1.2 for a general $n \in L_\infty(\Omega)$ the uniqueness in the two-dimensional case is not proven.*

6.2 Reconstruction methods for a constant background

This section is devoted to numerical methods for the reconstruction of the refractive index.

Let us consider the refraction index of a form

$$n(\mathbf{x}) = 1 + f(\mathbf{x}), \tag{6.2}$$

where we assume that

$$supp(f) \subset \Omega \subset\subset \mathbb{R}^2.$$

Without loss of generality we assume that $\Omega = B(R)$ for some R.

In this case the problem is to reconstruct the potential $f(\mathbf{x})$ from the data g_θ given on Γ^+ (see Figure 6.1). In the real applications the available data is known only for a finite sequence of $\theta_j, j = 1, ..., N$, i.e., only for the finite number of the incident plane waves u_i^j.

Over the years algorithms to solve the inverse scuttering problem were proposed, below we briefly describe some main ideas behind these algorithms

The first group has its origin in the *Born* and *Rytov approximations* [Devaney, Kak1988].

The Born approximation is based on the Lippmann-Schwinger equation (2.2.3), which in this case is

$$u(\mathbf{x}) = u_i(\mathbf{x}) + k^2 \int\limits_\Omega f(\mathbf{y}) u(\mathbf{y}) G(\mathbf{x}, \mathbf{y}) d\mathbf{y}.$$

Assuming that the scattered field is small compared to the incident we replace $u(\mathbf{y})$ on right-hand side by $u_i(\mathbf{y})$. Now putting the known data g_θ to the left-hand side we get the linear equation for $f(\mathbf{x})$:

$$g_\theta(\mathbf{x}) \simeq u_i(\mathbf{x}) + k^2 \int\limits_\Omega f(\mathbf{y}) u_i(\mathbf{y}) G(\mathbf{x}, \mathbf{y}) d\mathbf{y}.$$

The solution of this linear problem can be found for example by use of the least square method (see, e.g.,[Wübbeling1994]).

The Born approximation is based on the assumption that the scattered field is much smaller than incident. For the case of scattering on a homogeneous disk this condition can be expressed in terms of the diameter of the disk d, refractive index of the disk f and k as [Kak1988]:

$$dfk < \pi. \tag{6.3}$$

In the Rytov approximation the total field is represented in a form

$$u(\mathbf{x}) = \exp(\varphi(\mathbf{x})), \tag{6.4}$$

with the complex total phase $\varphi(\mathbf{x}) = \varphi_i(\mathbf{x}) + \varphi_s(\mathbf{x})$, where $u_i(\mathbf{x}) = \exp(\varphi_i(\mathbf{x}))$. The assumption in the Rytov approximation is that the scattered phase φ_s changes slowly over one wavelength. Inserting (6.4) into the Helmholtz equation and doing some trivial algebraic computations we get the approximation for the complex phase of the scattered field

$$\varphi_s(\mathbf{x}) \simeq \frac{1}{u_i(\mathbf{x})} \int\limits_{\mathbb{R}^2} u_i(\mathbf{y}) f(\mathbf{y}) G(\mathbf{x}, \mathbf{y}) d(\mathbf{y}).$$

Again we get a linear equation for $f(\mathbf{x})$.

The Rytov approximation is valid under less restrictive assumptions than the Born approximation. It is valid when the phase change over a single wavelength is small (see, e.g., [Kak1988]):

$$\left(\frac{\nabla \varphi_s}{k} \right) < f.$$

The Born and Rytov approximations produce the same result in the case when both are valid (see [Kak1988]).

The case where k is large is a challenge. But some methods to deal with this case were developed. Most of them are based on the propagation-backpropagation (PBP) algorithm proposed by Natterer and Wübbelling [Natterer1995] and adopted in [Natterer2004].

The PBP method is iterative in the nature. It defines f from the knowledge of $v_\theta = (g_\theta - u_i^j)/u_i^j$, which is the scattered field u_s scaled by the incident u_i^j.

We describe the PBP algorithm after [Natterer1995]. Consider a square Q_j represented together with its boundaries Γ_j,Γ_j^- and Γ_j^+ on the Figure 6.2. Let R_j be a so-called *propagation operator*, defined by

$$\begin{array}{l} R_j : L^2(Q_j) \to L^2(\Gamma_j^+) \\ f \mapsto v_{\theta_j}|_{\Gamma_j^+} \end{array} \tag{6.5}$$

$$\begin{array}{l} \Delta v_{\theta_j} + 2ik\Theta\nabla v_{\theta_j} + k^2 f v_{\theta_j} = -k^2 f \\ \\ v_{\theta_j} = g_{\theta_j} \quad \text{on} \quad \Gamma_j^- \cup \Gamma_j^+ \\ \\ \dfrac{\partial}{\partial \nu} v_{\theta_j} = \dfrac{\partial}{\partial \nu} g_{\theta_j} \quad \text{on} \quad \Gamma_j^-, \end{array} \tag{6.6}$$

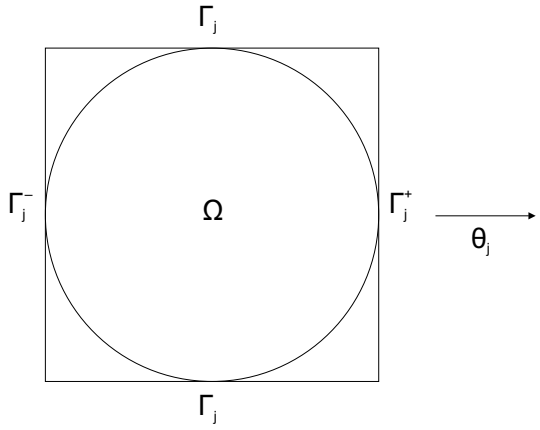

Figure 6.2: the basic geometry of the PBP method.

where ν is the interior normal to ∂Q_j. Thus, with $g_j = g_{\theta_j}|_{\Gamma_j^+}$ we have

$$R_j(f) = g_j \quad j = 0, ..., N-1. \tag{6.7}$$

This nonlinear system is solved by iterations. Taking the initial guess f^0 the approximation f^{p+1} is given by $f^{p+1} = f^p - \omega d^p$, where ω is a relaxation factor and d^p is an approximation to the minimal norm solution of

$$R_j(d^p + f^p) = g_j, \quad j = p \bmod N.$$

The approximation d^p is obtained from the linearization of (6.7).The resulting iteration step is follows

$$f^{p+1} = f^p - \omega R_j'(f^p)^*(g_j - R_j(f^p)), \quad j = p \bmod N.$$

Here the *back-propagator* $R_j'(f)^*$ is defined by

$$\begin{aligned} &R_j'(f)^* : L^2(\Gamma_j^+) \to L^2(Q_j) \\ &g_j \mapsto k^2(1 + \overline{v}_{\theta_j})z \end{aligned} \tag{6.8}$$

$$\begin{aligned} &\Delta z + 2ik\boldsymbol{\theta}_j \nabla z + k^2 \overline{f} z = 0 \quad \text{in} \quad Q_j \\ &z = 0 \quad \text{on} \quad \Gamma_j^- \cup \Gamma_j \\ &\frac{\partial z}{\partial \nu} = g_j \quad \text{on} \quad \Gamma_j^-. \end{aligned} \tag{6.9}$$

The PBP method was adopted in [Caponnetto1998] for the geometrical-optics approximation. Author proposed an PBP algorithm analogous to

presented above to reconstruct the potential f from the knowledge of the eikonal ϕ_j over a line perpendicular to the direction of the incident plane wave propagation.

In the next section we propose a new reconstruction algorithm for the case when k is large of a different nature. It is based directly on the geometrical-optics approximation.

6.3 Reconstruction of the perturbation of refractive index

This section is devoted to a new reconstruction algorithm based on the geometrical-optics approximation.

We mention first that in the medical applications a typical biological material is inhomogeneous, but, by excluding fat, the variations of of sound velocity are so small (e.g., 0.11%, see [Angelsen2000]) that they can safely be ignored. However, in the presence of inclusions (for example, tumors) the biological material is inhomogeneous enough to scatter ultrasound.

Thus, it is natural to consider the inverse scattering problem where the medium examination is a small perturbation of a known background.

Let the refractive index $n_0(\mathbf{x})$ be a known function. The task is to reconstruct the perturbed refractive index $n = n_0 + n_1$ from the knowledge of the wave fields u_0 and u, corresponding to these refractive indexes.

On the more formal level formulation of the problem is follows. Consider the Helmholtz equation

$$\Delta u_0(\mathbf{x}) + k^2 n_0(\mathbf{x}) u_0(\mathbf{x}) = 0 \tag{6.10}$$

together with the perturbed one

$$\Delta u(\mathbf{x}) + k^2 n(\mathbf{x}) u(\mathbf{x}) = 0, \tag{6.11}$$

where the scattered parts of the solutions u and u_0 satisfy the radiating condition (2.2) with the incident field $u_i(\mathbf{x}) = \exp(ik\boldsymbol{\theta}\mathbf{x})$ in both cases. Let $n(\mathbf{x}) = n_0(\mathbf{x}) = const$ for $\mathbf{x} \in \mathbb{R}^2 \setminus \Omega$, where $\Omega \subset\subset \mathbb{R}^2$. Assume that we have measured fields u and u_0 for the sufficiently many incident waves u_i and the refractive index n_0 is known. The task is to reconstruct n from these data.

A natural reconstruction idea based on the eikonal approximation was proposed by Palamodov [Palamodov1996].

Theorem 6.3.1 *Let the non-trapping condition (4.1.1) be satisfied. Denote $n_0(\mathbf{x}) - n(\mathbf{x}) = h(\mathbf{x})/k$. Let $\Omega \subset D$, where the domain D contains no caustic. Then the solution of the perturbed Helmholtz equation (6.11) admits the following expansion in D*

$$u(\mathbf{x}) = \frac{1}{J(\mathbf{x})} \exp(i[k\phi(x) - \int_0^{s_0} h(\gamma_0(s))ds]) + v(\mathbf{x}, k), \tag{6.12}$$

where γ_0 is the ray corresponding to n_0, which comes to $\mathbf{x}$: $\gamma_0(s_0) = \mathbf{x}$ and

$$v(\mathbf{x}, k) = O(k^{-1})(||n_0||^{1+\varepsilon} + ||n_0 - n||^{1+\varepsilon})$$

for an arbitrary $\varepsilon > 0$.

This theorem gives a reconstruction algorithm supposing that there is no caustic in the domain of interest. From the measured data g_θ we can recover the factor $\exp(-i\int_0^{s_0} h(\gamma_0(s))ds)$, where the integral is taken over a ray corresponding to the non perturbed refractive index. Assuming that the noise is low we get the approximation of the values of the integral $\int_0^{s_0} h(\gamma_0(s))ds$ up to $2m\pi$, where m is a integer. Thus, the inverse scattering problem is reduced to the problem of reconstruction the function f from integrals over rays.

The theorem is not proven by now. We have proven some estimates on the error function v (see Sections 4.2 and 5.2), which are listed below.

Consider the refractive index of a form $n(\mathbf{x}) = 1 + f(\mathbf{x})$, where we assume that $f \in C^1$,$|f(\mathbf{x})| < 1$,$|\nabla f| < M < \infty$, $supp(f) \subset \Omega \subset\subset \mathbb{R}^2$ and $\Omega \subset D$, where the domain D contains no caustic. Denote $\varepsilon = ||f||_\Omega$.

For the solution of the Helmholtz equation (2.1) with the radiating condition (2.2) we have

$$u(\mathbf{x}) = \frac{1}{\sqrt{J(\mathbf{x})}} \exp(ik\phi(\mathbf{x})) + v(\mathbf{x}),$$

where v allows the estimate for $B \cap D$ with $B = [-R, R] \times [0, \infty)$, $R > 0$ (4.15)

$$||v_{\zeta' k}(\mathbf{x})||^2_{L_2(-R,R)} \leq \frac{C}{k^2\zeta'^2} ||\Delta \left(\sqrt{J(\mathbf{x})}\right)^{-1} ||^2_{L_2(B)}, \tag{6.13}$$

with positive constants ζ' and C.

Moreover we have proven (5.5) that

$$\phi(\mathbf{x}) = \phi_0(\mathbf{x}) - \frac{1}{2}\int_{\gamma_0} f(\gamma_0(s))ds + O(\varepsilon^2), \tag{6.14}$$

where ϕ_0 is the non perturbed eikonal and integral is taken over the non perturbed ray γ_0 coming to $\mathbf{x}$.

In the case of the constant background $\phi_0 = \mathbf{x}\boldsymbol{\theta}$ where $\boldsymbol{\theta}$ is the direction of the incident plane wave. The rays are straight lines, thus, the integral of f is taken over the straight line parallel to $\boldsymbol{\theta}$ and passing through $\mathbf{x}$.

Since the rays of the non-perturbed medium are straight lines we get the expansion for the Radon transform of the perturbation f:

$$\int_{-\infty}^{0} f ds \simeq \frac{1}{ik} \log \frac{g_\theta}{|g_\theta|} - \mathbf{x}\boldsymbol{\theta}. \tag{6.15}$$

That is, one can recover the perturbation f from the measurement of the wave field u, since the Radon transform is invertible. In the next section we give some reconstruction examples.

6.4 Numerical examples

To test the algorithm presented in the previous section we use examples, which allow the analytical solution of the direct scattering problem. That is we consider the scattering on a homogeneous disk and on two concentric disks.

First we attempt the scattering on the homogeneous disk of radius $R = 1$ (which corresponds to $R = 64$ measured in the lattice points), with the refractive index $n(\mathbf{x}) = 1.01$ inside, in a homogeneous medium with $n(\mathbf{x}) = 1$ outside the disk. We compare the results with different values of the wave number k: $k = 25$ (Figures 6.3, 6.4, 6.5), $k = 100$ (Figures 6.6, 6.7, 6.8) and $k = 200$ (Figures 6.9, 6.10, 6.11). The imaginary part of the approximation (6.15) is very small (nearly zero). For this reason we do not show it every time. We see that with increasing of k the reconstruction becomes better. We remind that the case of big values of k can not be treated by the Born approximation, because the condition (6.3) is not satisfied.

Further we fix $k = 200$ and change the refractive index of the disk: $n(\mathbf{x}) = 1.05$ (Figures 6.12, 6.13, 6.14) and $n(\mathbf{x}) = 1.1$ (Figures 6.15, 6.16, 6.17). The refractive index $n = 1.01$ is presented already (see Figures 6.9, 6.10, 6.11). The disk radius remains $R = 1$ ($R = 64$ in the terms of lattice points). Again we show the imaginary part only for the approximation (6.15). In this case the increasing of the refractive index makes the reconstruction worse.

The last example is the scattering on two concentric disks. We consider disks of radii $R_1 = 1$ and $R_2 = 0.5$ (which corresponds in terms of lattice points to 64 and 32 respectively). The value of the refractive index $n(\mathbf{x})$ is 1.1 inside the inner disk, 1.01 inside the ring between two circles and 1 outside the outer disk. We compare two different wave numbers $k = 150$ and $k = 100$. Again we see that the reconstruction for $k = 150$ (Figures 6.21, 6.22, 6.23) is better than it is for $k = 100$ (Figures 6.18, 6.19, 6.20).

We use in each case 180 projections, i.e., 180 incident waves with equal spacing between direction angles.

The increasing of the reconstruction quality with the increasing of k and its decreasing when the refractive index grows are reasoned by the estimates (6.13, 6.14).

Note, that all pictures on the same page have identical colourbars, the latter however can change from page to page.

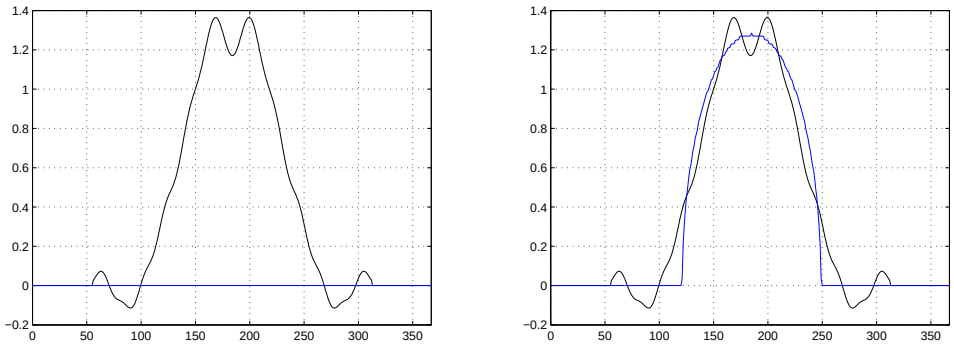

Figure 6.3: $k = 25$, $f(\mathbf{x}) = 0.01$. Left: the real (black) and imaginary (blue) part of the approximation (6.15), right: the real part of (6.15) (black) and the exact radon transform (blue).

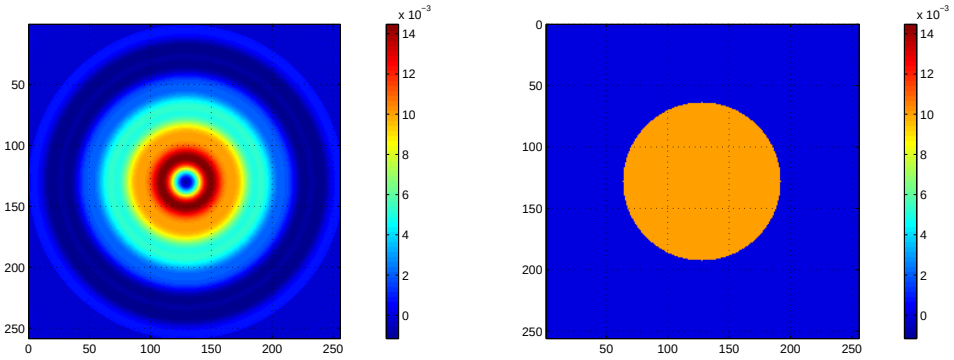

Figure 6.4: $k = 25$, $f(\mathbf{x}) = 0.01$. Left: the reconstruction of the function $f(\mathbf{x})$ (real part), right: the exact function

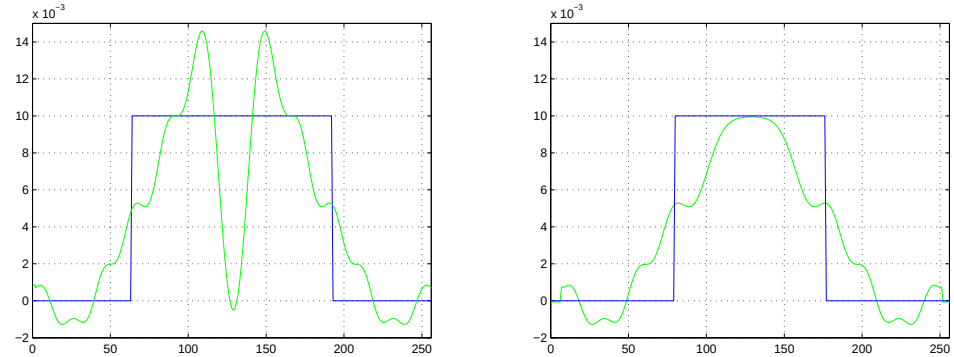

Figure 6.5: $k = 25$, $f(\mathbf{x}) = 0.01$. Left: the cross-section of the reconstruction 6.4 (green) and the cross-section of the exact function for the horizontal 128 (the center of the disk), right: the cross-section of the reconstruction (green) and the cross-section of the exact function for the horizontal 170.

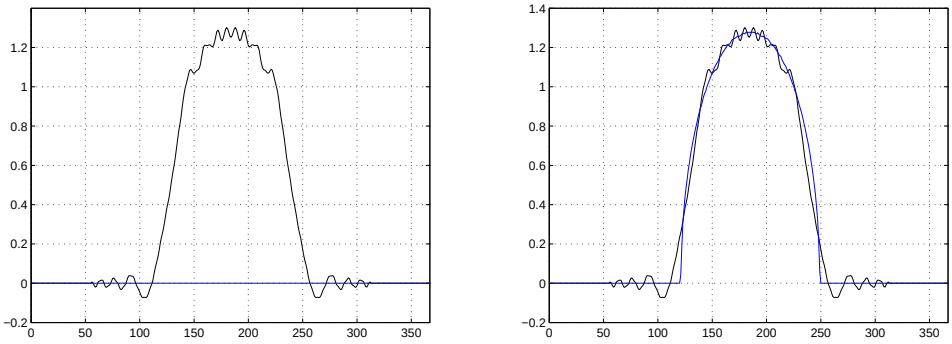

Figure 6.6: $k = 100$, $f(\mathbf{x}) = 0.01$. Left: the real (black) and imaginary (blue) part of the approximation (6.15), right: the real part of (6.15) (black) and the exact radon transform (blue).

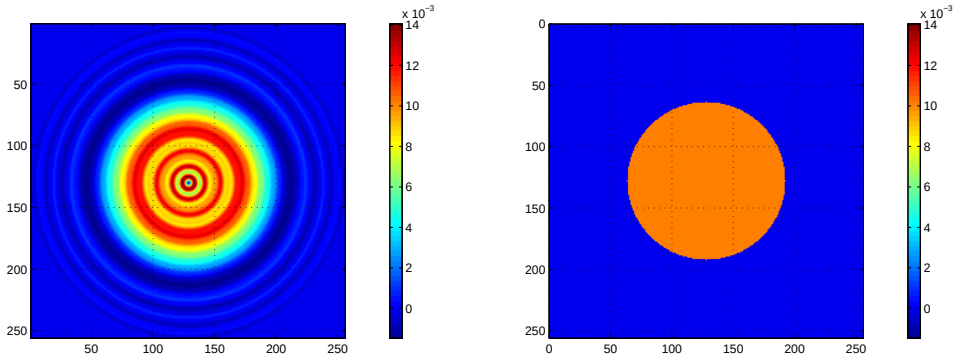

Figure 6.7: $k = 100$, $f(\mathbf{x}) = 0.01$. Left: the reconstruction of the function $f(\mathbf{x})$ (real part), right: the exact function

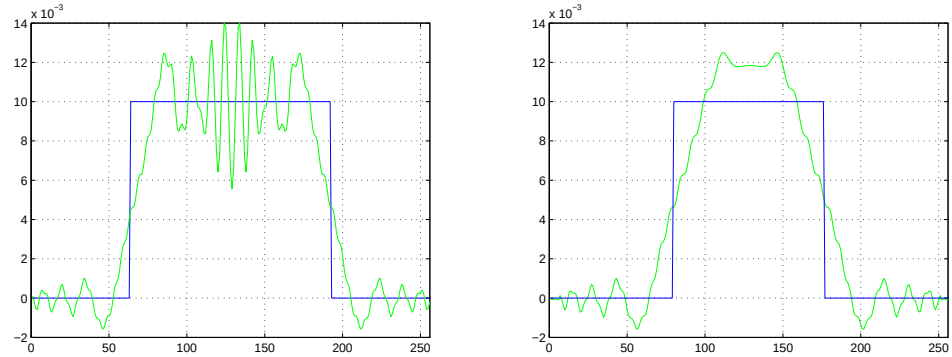

Figure 6.8: $k = 100$, $f(\mathbf{x}) = 0.01$. Left: the cross-section of the reconstruction 6.7 (green) and the cross-section of the exact function for the horizontal 128 (the center of the disk), right: the cross-section of the reconstruction (green) and the cross-section of the exact function for the horizontal 170.

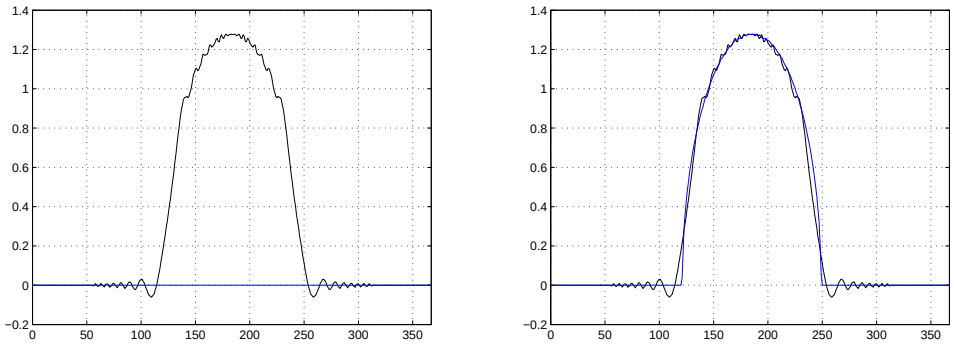

Figure 6.9: $k = 200$, $f(\mathbf{x}) = 0.01$. Left: the real (black) and imaginary (blue) part of the approximation (6.15), right: the real part of (6.15) (black) and the exact radon transform (blue).

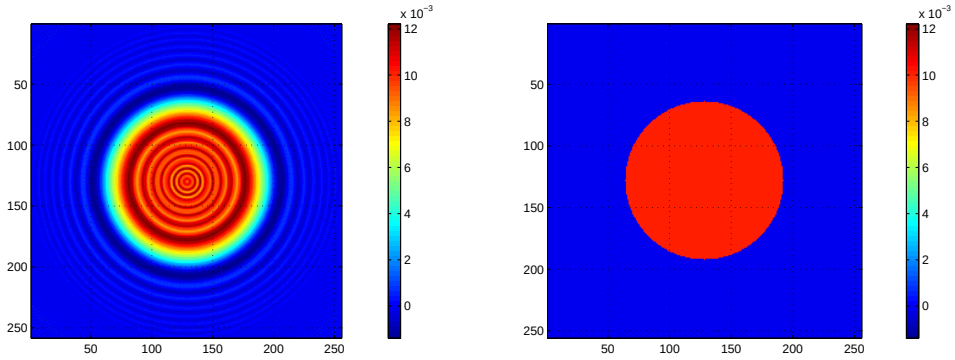

Figure 6.10: $k = 200$, $f(\mathbf{x}) = 0.01$. Left: the reconstruction of the function $f(\mathbf{x})$ (real part), right: the exact function

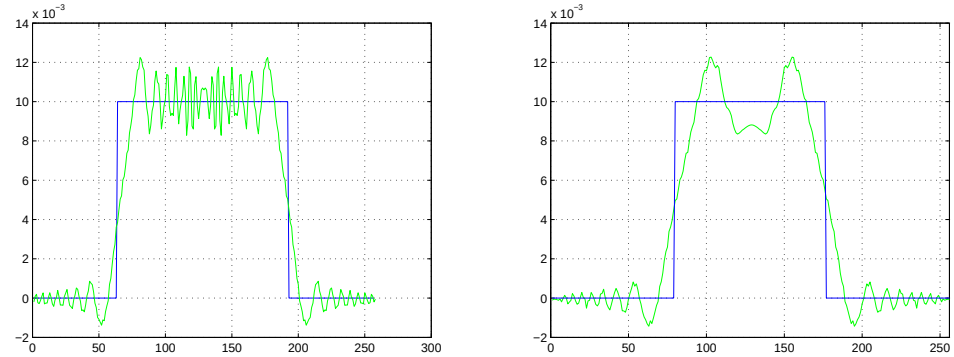

Figure 6.11: $k = 200$, $f(\mathbf{x}) = 0.01$. Left: the cross-section of the reconstruction 6.10 (green) and the cross-section of the exact function for the horizontal 128 (the center of the disk), right: the cross-section of the reconstruction (green) and the cross-section of the exact function for the horizontal 170.

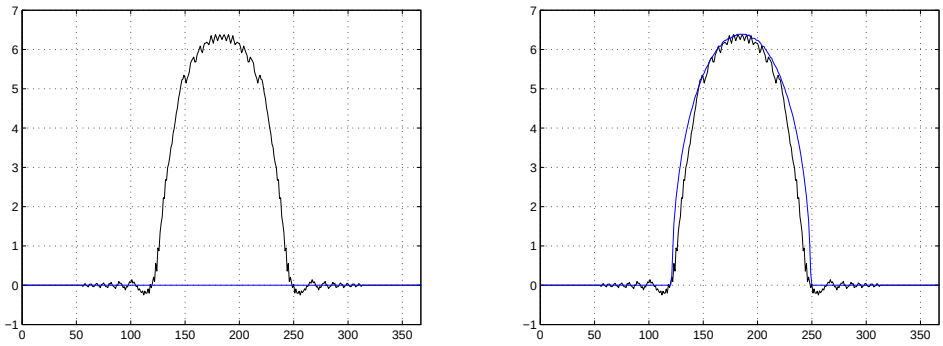

Figure 6.12: $k = 200$, $f(\mathbf{x}) = 0.05$. Left: the real (black) and imaginary (blue) part of the approximation (6.15), right: the real part of (6.15) (black) and the exact radon transform (blue).

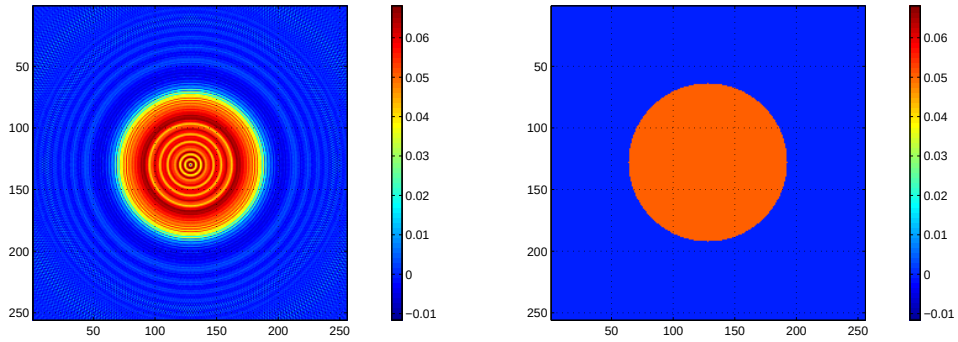

Figure 6.13: $k = 200$, $f(\mathbf{x}) = 0.05$. Left: the reconstruction of the function $f(\mathbf{x})$ (real part), right: the exact function

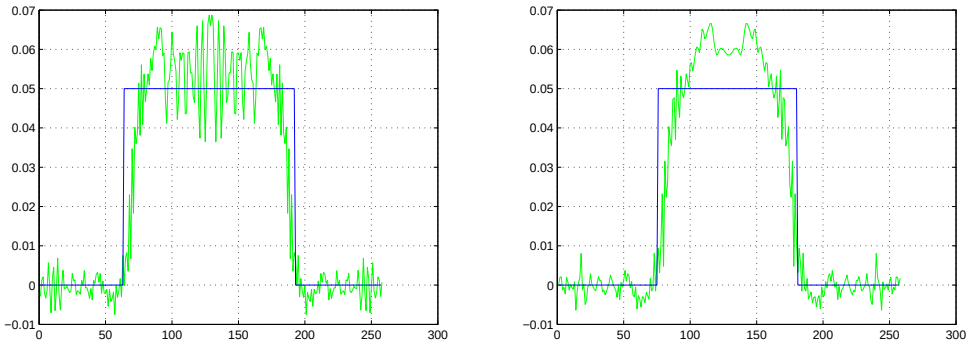

Figure 6.14: $k = 200$, $f(\mathbf{x}) = 0.05$. Left: the cross-section of the reconstruction 6.13 (green) and the cross-section of the exact function for the horizontal 128 (the center of the disk), right: the cross-section of the reconstruction (green) and the cross-section of the exact function for the horizontal 170.

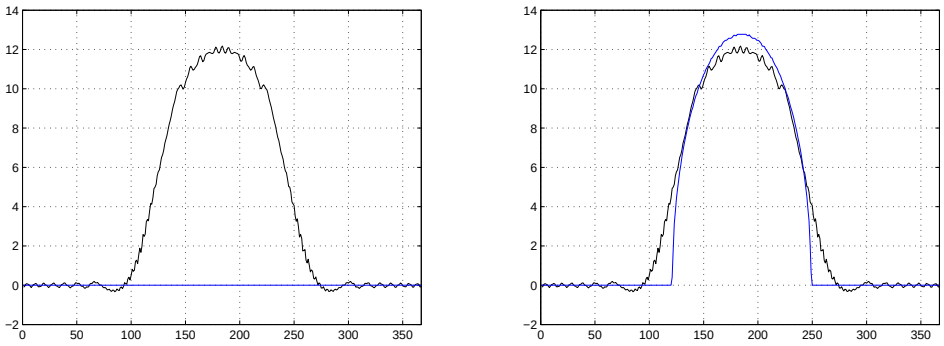

Figure 6.15: $k = 200$, $f(\mathbf{x}) = 0.1$. Left: the real (black) and imaginary (blue) part of the approximation (6.15), right: the real part of (6.15) (black) and the exact radon transform (blue).

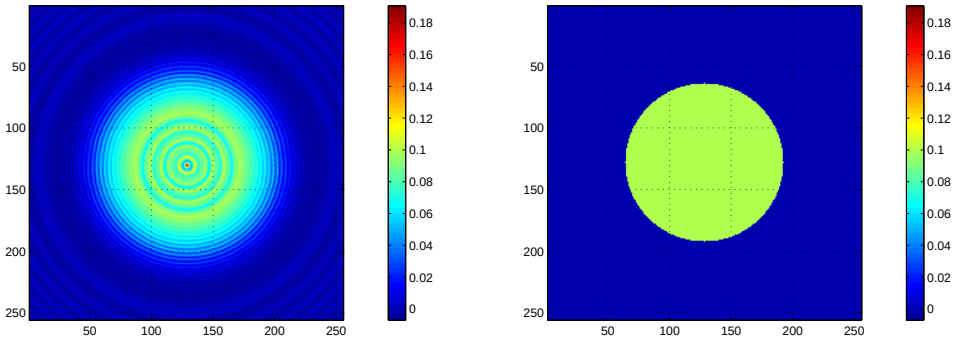

Figure 6.16: $k = 200$, $f(\mathbf{x}) = 0.1$. Left: the reconstruction of the function $f(\mathbf{x})$ (real part), right: the exact function

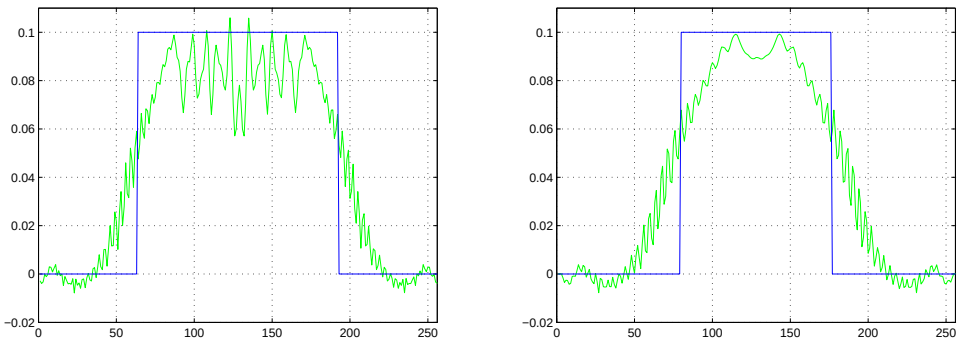

Figure 6.17: $k = 200$, $f(\mathbf{x}) = 0.1$. Left: the cross-section of the reconstruction 6.16 (green) and the cross-section of the exact function for the horizontal 128 (the center of the disk), right: the cross-section of the reconstruction (green) and the cross-section of the exact function for the horizontal 170.

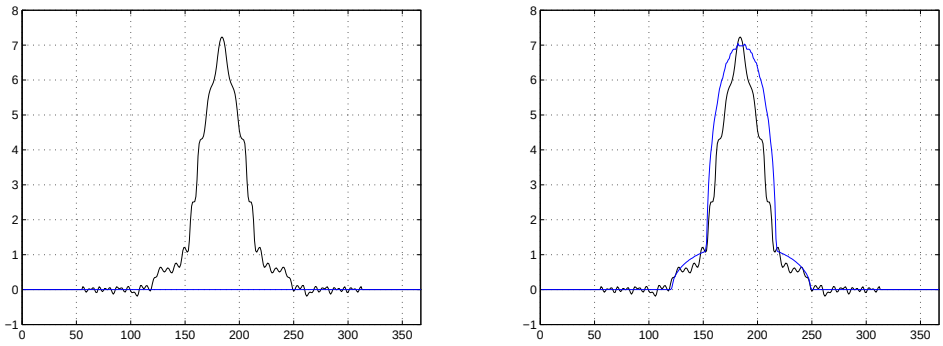

Figure 6.18: $k = 100$, $f_1(\mathbf{x}) = 0.01$, $f_2(\mathbf{x}) = 0.1$. Left: the real (black) and imaginary (blue) part of the approximation (6.15), right: the real part of (6.15) (black) and the exact radon transform (blue).

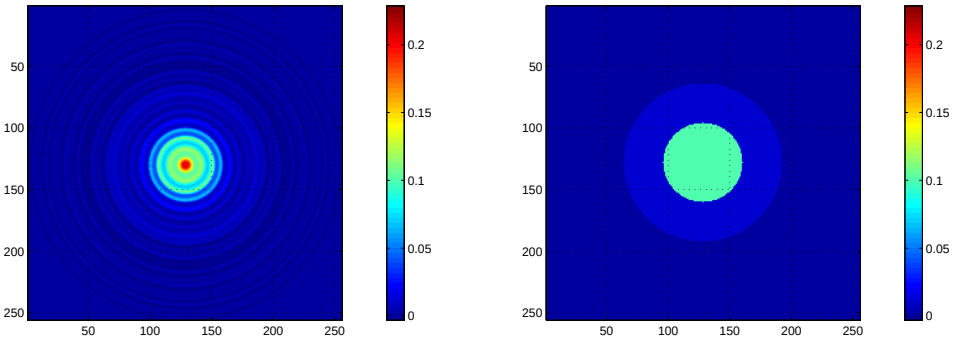

Figure 6.19: $k = 100$, $f_1(\mathbf{x}) = 0.01$, $f_2(\mathbf{x}) = 0.1$. Left: the reconstruction of the function $f(\mathbf{x})$ (real part), right: the exact function

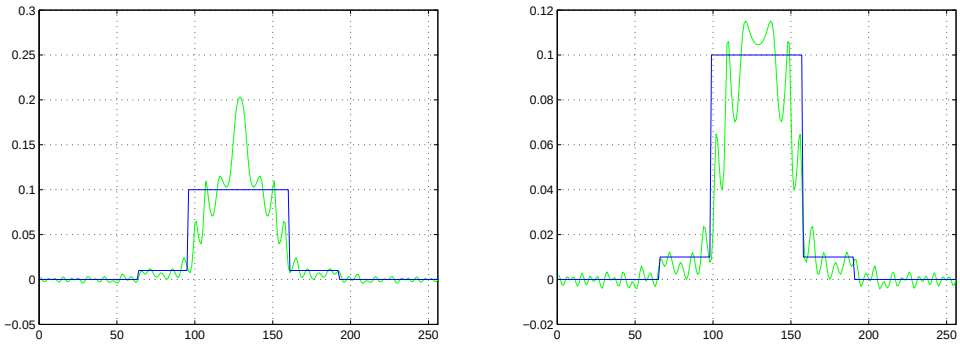

Figure 6.20: $k = 100$, $f_1(\mathbf{x}) = 0.01$, $f_2(\mathbf{x}) = 0.1$. Left: the cross-section of the reconstruction 6.19 (green) and the cross-section of the exact function for the horizontal 128 (the center of the disk), right: the cross-section of the reconstruction (green) and the cross-section of the exact function for the horizontal 140.

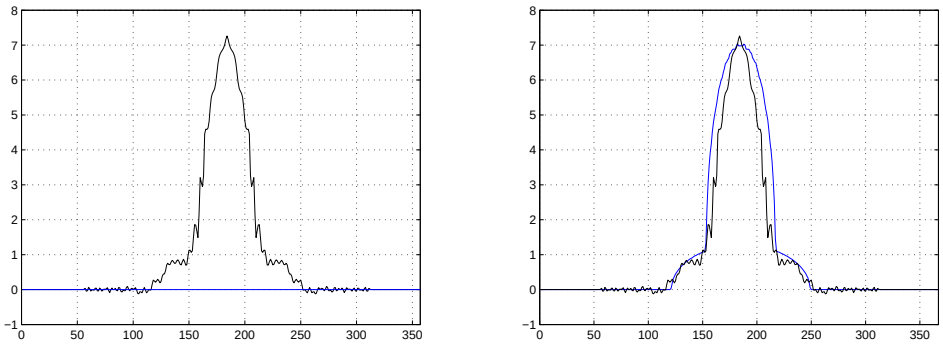

Figure 6.21: $k = 150$, $f_1(\mathbf{x}) = 0.01$, $f_2(\mathbf{x}) = 0.1$. Left: the real (black) and imaginary (blue) part of the approximation (6.15), right: the real part of (6.15) (black) and the exact radon transform (blue).

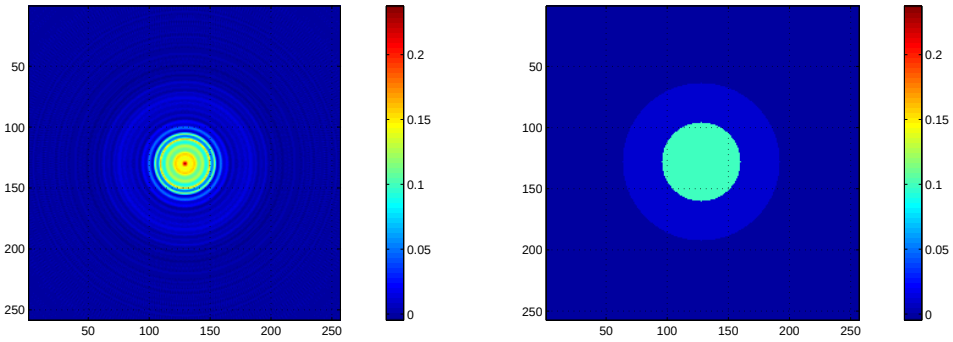

Figure 6.22: $k = 150$, $f_1(\mathbf{x}) = 0.01$, $f_2(\mathbf{x}) = 0.1$. Left: the reconstruction of the function $f(\mathbf{x})$ (real part), right: the exact function

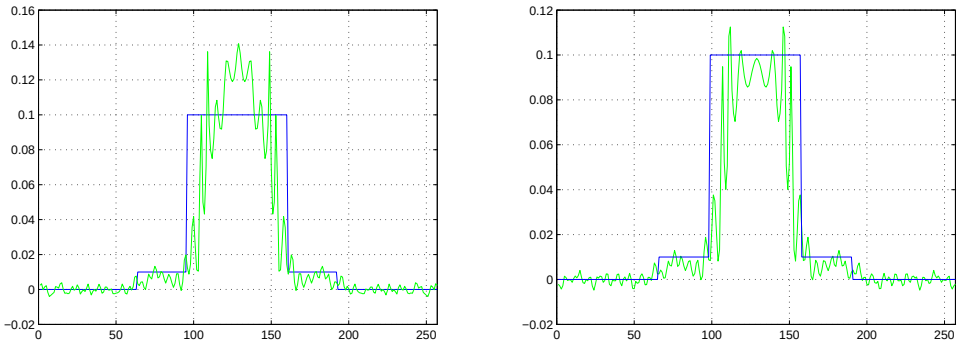

Figure 6.23: $k = 150$, $f_1(\mathbf{x}) = 0.01$, $f_2(\mathbf{x}) = 0.1$. Left: the cross-section of the reconstruction 6.22 (green) and the cross-section of the exact function for the horizontal 128 (the center of the disk), right: the cross-section of the reconstruction (green) and the cross-section of the exact function for the horizontal 140. Note that the maximum grid values are different for these two graphs.

Bibliography

[Abgrall1999] R Abgrall and J.-D. Benamou. Big ray-tracing and eikonal solver on unstructured grids: Application to the computation of a multi-valued traveltime field in the Marmousi model. *Geophysics*, **64**, 230–239 (1999).

[Abramowitz1965] M. Abramowitz and I. A. Steugun. *Handbook of Mathematical Functions with Formulas, Graphs, and Mathematical Tables*. Dover Publications (1965).

[Angelsen2000] Bjorn A.J. Angelsen. *Ultrasound imaging, Vol. I*. Emantec, Norway (2000).

[Arnold1989] V. I. Arnold. *Mathematical methods in classical mechanics*. Springer (1989).

[Babich1979] V. M. Babich and N. Ya. Kirpichnikova. *The boundary-layer method in diffraction problems*. Springer-Verlag, Berlin-New York (1979).

[Babich1991] V. M. Babich and V. S. Buldyrev. *Short-Wavelength Diffraction Theory*. Springer-Verlag (1991).

[Beals1986] R. Beals and R. R. Coifman. The D-bar approach to inverse scattering and nonlinear evolutions. *Physica D Nonlinear Phenomena*, **18**, 242–249 (1986).

[Benamou] J.-D. Benamou. *Computation of multi-valued traveltimes in the Marmousi model*. http://www-rocq.inria.fr/∼benamou/testproblem.html.

[Bolomey1989] J. Bolomey. Recent European Developments in active microwave imaging for industrial, scienftific and medical application. *IEEE Trans. Microwave Theory Tech.*, **37**, 2109–2117 (1989).

[Born1999] M. Born and E. Wolf. *Principles of Optics*. Cambridge University Press (1999).

[Borovikov1994] V. A. Borovikov. *Uniform stationary phase method*. Series on Electromagnetic Waves (1994).

[Borup1992] D.T. Borup, Johnson S. A., Kim, W.W, and Berggren M.J. Nonperturbative diffraction tomography via Gauss-Newton iteration applied to the scattering integral equation. *Ultrasonic Imaging*, **14**, 69–85 (1992).

[Bruns1895] H Bruns. Das Eikonal. Zusatz. *Leipz. Abh.*, **XXI**, 325–436 (1895).

[Burq2002] N. Burq. Semi-classical estimates for the resolvent in non trapping geometries. *Int. Math. Res. Not.*, **5**, 221–241 (2002).

[Caponnetto1998] A. Caponnetto. *Tomographic methods and applications*. PhD thesis, Facoltà di Scienze Matematiche, Fisiche e Naturali, Università degli Studi di Genova (1998).

[Cerveny1982] V. Cerveny and J. Jech. Linearized solutions of kinematic problems of seismic body waves in inhomogeneous slightly anisotropic media. *Geophys. J. Int*, **51**, 96–104 (1982).

[Colton1992] D. Colton and R. Kress. *Inverse Acoustic And Electromagnetic Scattering Theory*. Springer-Verlag (1992).

[Devaney] A.J. Devaney. A filtered backpropagation algorithm. for diffraction tomography. *Ultrasonic imaging*, **4**.

[Engquist2003] B. Engquist and O. Runborg. Computational high frequency wave propagation. *Acta Numerica*, **53**, 181–266 (2003).

[Farra1987] V. Farra and R. Madariaga. Seismic waveform modeling in heterogeneous media by ray perturbation theory. *J.geophys.Res.*, **92**, 3697–3712 (1987).

[Farra1989a] V. Farra. Ray perturbation theory for a heterogeneous hexagonal anisotropic medium. *Geophys.J. Int.*, **99**, 723–738 (1989).

[Farra1989b] V. Farra, J. Virieux, and R. Madariaga. Ray perturbation theory for interfaces. *Geophys. J. Int*, **99**, 377–390 (1989).

[Farra1999] V. Farra. Computation of second-order traveltime perturbation by Hamiltonian ray theory. *Geophys.J.Int.*, **136**, 205–217 (1999).

[Gilbarg2001] D. Gilbarg and N. S. Trudinger. *Elliptic partial differential equations of second order*. Springer (2001).

[Hähner1996] P. Hähner. A periodic Faddeev-type solution operator. *J.differential Equations*, **128**, 300–308 (1996).

[Hähner1998] P. Hähner. *On acoustic, electromagnetic and elastic scattering problems in inhomogeneous media*. Habilititationsschrift, Göttingen (1998).

[Hamilton1982] R. S. Hamilton. The inverse function theorem of Nash and Moser. *Bull. Amer. Math. Soc.*, **7**, 65–222 (1982).

[Hörmander1994] L. Hörmander. *The analysis of linear partial differential operators 1*. Springer-Verlag (1994).

[Kak1988] A. C. Kak and M. Slaney. *Principles Of Computerized Tomographic Imaging*. IEEE Press (1988).

[Kravtsov1999] Yu. A. Kravtsov and Orlov Yu. I. *Caustics, Catastrophes and Wave Fields*. Springer-Verlag (1999).

[Kucherenko1969] V. V. Kucherenko. Quasiclassical asymptotics of a point-source function for the stationary Schrödinger equation. *Theoret. Math. Phys.*, **1**, 294–310 (1969).

[Kupradze1934] V. Kupradze. Über das "Ausstrahlungsprinzip" von A. Sommerfeld. *C. R. Acad. Sc. URSS*, **2**, 52–58 (1934).

[Luneberg1944] R.K. Luneberg. *Mathematical Theory of Optics.* Brown University, Provicence, R. I. (1944).

[Magnus1949] W. Magnus. Fragen der Eindeutigkeit und des Verhaltens im Unendlichen für Lösungen von $\Delta u + k^2 u = 0$. *Abh. Math. Semin. Univ. Hamb.*, **16**, 77–94 (1949).

[Miranker1957] W.L. Miranker. Uniqueness and representations theorems for solutions of $\Delta u + k^2 u = 0$ in infinite domains. *J. Math. Mech.*, **6**, 847–858 (1957).

[Morgan1958] S Morgan. General Solution of the Luneberg Lens Problem. *J. Appl. Phys.*, **29**, 1358–1368 (1958).

[Nachman1988] A. Nachman. Global uniqueness for a two-dimensional inverse boundary value problem. *Ann. of Math.*, **143**, 71–96 (1988).

[Natterer1995] F. Natterer and F. Wübbeling. A propagation-backpropagation method for ultrasound tomography. *Inverse Probl.*, **11**, 1225–1232 (1995).

[Natterer1997] F. Natterer. An initial value approach to the inverse Helmholtz problem at fixed frequency. *Engl, Heinz W. (ed.) et al.,Inverse Problems in medical imaging and nondestructive testing. Proceedings of the conference in Oberwolfach*, , 159–167 (1997).

[Natterer2004] F. Natterer and F. Wübbeling. *Marching schemes for inverse acoustic scattering problems.* http://wwwmath1.uni-muenster.de/num/Preprints/2004/ (2004).

[Nayfeh1973] A. H. Nayfeh. *Perturbation methods.* Wiley (1973).

[Novikov1987] R. Novikov and G. Henkin. The $\overline{\partial}$-equation in the multidimensional inverse scattering problem. *Russian Math. Surveys*, **42**, 109–180 (1987).

[Palamodov1996] V. P. Palamodov. Ray methods in diffraction tomography (1996).

[Pauen2000] R. Pauen. Non-trapping conditions and local energy decay for hyperbolic problems. *Konstanzer Schriften in Mathematik und Informatik*, **132**, 1–143 (2000).

[Pintavirooj2004] C. Pintavirooj, A. Romputtal, A. Ngamlamiad, W. Withayachumnankul, and K. Hamamoto. Ultrasonic refractive index tomography. *Journal of WSCG*, **12**, 333–340 (2004).

[Rayleigh1945] J. Rayleigh and B. Strutt. *The Theory of Sound, 2d ed.* Dover Publications, N. Y. (1945).

[Rellich1943] F. Rellich. Über das asymptotische Verhalten der Lösungen von $\Delta u + \lambda u = 0$ in unendlichen Gebieten. *Jahresbericht der Deutsch. Math. Ver.*, **53**, 57–65 (1943).

[Smirnov1972] V. I. Smirnov. *Lehrgang der höheren Mathematik.* Deutscher Verlag der Wissenschaften (1972).

[Snieder1992] R. Snieder and M. S. Sambridge. Ray perturbation theory for travel times and raypaths in 3-D heterogeneous media. *Geophys. J. Int.*, **109**, 294–322 (1992).

[Sommerfeld1912] A. Sommerfeld. Die *Green*sche Funktion der Schwingungsgleichung. *[J] Deutsche Math.-Ver.*, **21**, 309–353 (1912).

[Tichonov1985] A. N. Tichonov, A. B. Vasil'eva, and A. G. Sveshnikov. *Differential equations*. Springer-Verlag (1985).

[Vainberg1975] B. R. Vainberg. On the short wave asymptotic behaviour of solutions of stationary problems and the asymptotic behaviour as $t \to \infty$ of solutions of non-stationary problems. *Russ. Math. Surv.*, **30**, 1–58 (1975).

[Vainberg1989] B. R. Vainberg. *Asymptotic methods in equations of mathematical physics.* Gordon and Breach Science Publishers, New York (1989).

[Versteeg1993] R. J. Versteeg. Sensitivity of prestack depth migration to the velocity model. *Geophysics*, **58**, 873–882 (1993).

[Vladimirov1971] V.S. Vladimirov. *Equations Of Mathematical Physics*. Marcel Dekker Inc., New York (1971).

[Werner1960] P Werner. Zur mathematischen Theorie akustischer Wellenfelder. *Arch. Ration. Mech. Anal.*, **6**, 231–260 (1960).

[Wübbeling1994] F. Wübbeling. *Das direkte und das inverse streuproblem bei fester frequenz*. PhD thesis, Institut für Numerische Mathematik, Westfälische Wilhelms-Universität Münster (1994).